Development of a Model for the Ice Scraping Process

Iowa Department of Transportation Project HR 361

Final Report

by

W.A. Nixon, T.J. Gawronski, and A.E. Whelan

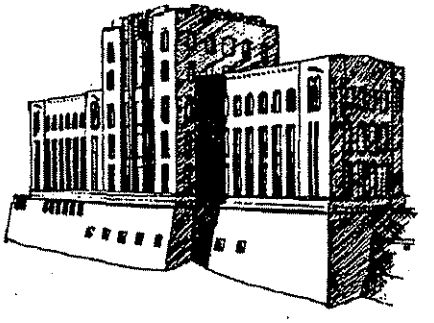

IIHR Technical Report No. 383

Iowa Institute of Hydraulic Research
College of Engineering
The University of Iowa
Iowa City IA 52242-1585

October 1996

ABSTRACT

A laboratory study has been conducted with two aims in mind. The first goal was to develop a description of how a cutting edge scrapes ice from the road surface. The second goal was to investigate the extent, if any, to which serrated blades were better than un-serrated or "classical" blades at ice removal.

The tests were conducted in the Ice Research Laboratory at the Iowa Institute of Hydraulic Research of the University of Iowa. A specialized testing machine, with a hydraulic ram capable of attaining scraping velocities of up to 30 m.p.h. was used in the testing.

In order to determine the ice scraping process, the effects of scraping velocity, ice thickness, and blade geometry on the ice scraping forces were determined. Higher ice thickness lead to greater ice chipping (as opposed to pulverization at lower thicknesses) and thus lower loads. Similar behavior was observed at higher velocities. The study of blade geometry included the effect of rake angle, clearance angle, and flat width. The latter were found to be particularly important in developing a clear picture of the scraping process. As clearance angle decreases and flat width increases, the scraping loads show a marked increase, due to the need to re-compress pulverized ice fragments.

The effect of serrations was to decrease the scraping forces. However, for the coarsest serrated blades (with the widest teeth and gaps) the quantity of ice removed was significantly less than for a classical blade. Finer serrations appear to be able to match the ice removal of classical blades at lower scraping loads. Thus, one of the recommendations of this study is to examine the use of serrated blades in the field. Preliminary work (by Nixon and Potter, 1996) suggests such work will be fruitful.

A second and perhaps more challenging result of the study is that chipping of ice is more preferable to pulverization of the ice. How such chipping can be forced to occur is at present an open question.

ACKNOWLEDGMENTS

This project was made possible by funding from the Iowa Department of Transportation, Project Number HR 361. This support is gratefully acknowledged.

The shop staff at IIHR, led by Mr. Jim Goss, made these experiments possible with their insight and assistance. Experiments were assisted by Ms. K. Hiranmayee. Thanks are extended to all these people.

The assistance and advice of Mr. Lee Smithson throughout the project has added significantly to the benefits obtained from the study.

TABLE OF CONTENTS

Chapter			Page
1	Introduction		1
2	Experimental Description		4
	2.1	Experimental Setup	5
		2.1.1 Ice Scraping Machine	5
		2.1.2 Load Cell Calibration	6
		2.1.3 Velocity Transducer Calibration	8
		2.1.4 Design and Manufacture of the Concrete Samples	8
	2.2	Parameters and Variables	9
	2.3	Typical Procedure	10
	2.4	Data Acquisition and Data Handling	11
3	Experimental Results		13
	3.1	Introduction	13
	3.2	Blade Variables	13
		3.2.1 Rake Angle Effect	13
		3.2.2 Clearance Angle Effect	15
		3.2.3 Flat Width Effect	17
		3.2.4 Blade Edge Effect	18
		3.2.5 Serrated Blades	19
	3.3	Ice Thickness Effect	21
	3.4	Velocity Effect	27
4	Discussion		30
	4.1	Introduction	30
	4.2	Rake Angle Effect	30
	4.3	Clearance Angle Effect	31
	4.4	Flat Width Effect	32
	4.5	Edge Effect	32
	4.6	Serrated Blades	32

4.7 Ice Thickness Effect 34

4.8 Velocity Effect 34

4.9 The Ice Scraping Process and Serrated Blades 34

5 Conclusions 36

Bibliography 38

Appendix

A Experimental Results 41

LIST OF FIGURES

Figure		Page
1.1	Definition of blade geometry variables	2
2.1	The cutting edge striking the ice	4
2.2	The ice scraping machine	5
2.3	The concrete block	6
2.4	The load cell calibration setup for x and y directions	7
2.5	The load cell calibration setup for z direction	8
2.6	Foam strips acting as dams	9
2.7	Cutting edge geometry of a classical blade	10
2.8	Cutting edge geometry with rectangular serration	10
3.1	Average vertical force vs thickness for various rake angles	14
3.2	Average horizontal force vs thickness for various rake angles	15
3.3	Average vertical force vs thickness for various clearance angles	16
3.4	Average horizontal force versus thickness for various clearance angles	16
3.5	Average vertical force vs thickness for various flat widths	17
3.6	Average horizontal force vs thickness for various flat widths	18
3.7	Average vertical force vs thickness for blades with various widths	19
3.8	Average horizontal force vs thickness for blades with various widths	19
3.9	Average vertical force vs thickness for serrated blades with various teeth sizes	19
3.10	Average horizontal force vs thickness for serrated blades with various teeth sizes	20
3.11	Averaged forces vs ice thickness for blade with a rake angle of 30°, clearance angle of 5°, and zero flat width	22
3.12	Maximum forces vs. ice thickness for blade with a rake angle of 30°, clearance angle of 5°, and zero flat width	22
3.13	Average forces vs. ice thickness for blade with a rake angle of 30°, clearance angle of 5°, and tooth size of 0.125 in.	23
3.14	Maximum forces vs. ice thickness for blade with a rake angle of 30°, clearance angle of 5°, and tooth size of 0.125 in.	23

3.15 Average forces vs. ice thickness for blade with a rake angle of 30°, clearance angle of 5°, and tooth size of 0.25 in. 24
3.16 Maximum forces vs. ice thickness for blade with a rake angle of 30°, clearance angle of 5°, and tooth size of 0.25 in. 24
3.17 Maximum forces vs. ice thickness for blade with a rake angle of 30°, clearance angle of 5°, and tooth size of 0.5 in. 25
3.18 Average forces vs. ice thickness for blade with a rake angle of 30°, clearance angle of 5°, and tooth size of 0.5 in. 25
3.19 Maximum forces vs. ice thickness for blade with a rake angle of 30°, clearance angle of 5°, and tooth size of 1 in. 26
3.20 Average forces vs. ice thickness for blade with a rake angle of 30°, clearance angle of 5°, and tooth size of 1 in. 26
3.21 Average forces vs. thickness for blade with a rake angle of 30°, clearance angle of 5°, and zero flat width 27
3.22 Maximum forces vs. thickness for blade with a rake angle of 30°, clearance angle of 5°, and zero flat width 28
3.23 Average forces vs. thickness for blade with a rake angle of 30°, clearance angle of 5°, and tooth size of 0.25 in. 28
3.24 Maximum forces vs. thickness for blade with a rake angle of 30°, clearance angle of 5°, and tooth size of 0.25 in. 29

4.1 Directions of ice chips for blunt and angled blades 31
4.2 Side view of a serrated blade (0.25 in.) surface after a run 33
4.3 Side view of a serrated blade (0.5 in.) surface after a run 33
4.4 Ice failure modes 35

Chapter 1
Introduction

More than half of the States in the United States experience winter weather each year of sufficient severity to create hazardous situations. Freezing rains and compacted snow often accumulate in winter on the highways and roads creating dangerous and fatal conditions for road users. The accidents caused by these conditions carry both a societal and an economic cost, which can be considerable (Hanbali, 1994). In addition to safety concerns, it is clear that ensuring good road conditions in the winter has a positive economic benefit. The procedure of Just-In-Time manufacturing has gained wide acceptance in U.S. industry, and requires not so much a low average transit time between locations, but a small standard deviation on that average transit time for best results (Forkenbrock et al., 1994). Such a low standard deviation is best obtained by ensuring good winter maintenance practice. The means for ensuring good road conditions (typically termed "bare pavement" conditions) traditionally comprise salting, sanding and scraping in the United States. Other countries do not require bare pavement conditions for some or most of their roads. This is particularly true in the Scandinavian countries and in Japan.

Salt (Sodium Chloride, typically in the form of rock salt) is applied to roads because it depresses the freezing point of water, thus causing ice and snow to melt. It is the most widely used deicer and is much cheaper than all other deicers. Sand is used to raise the friction coefficient between the vehicle tires and the road. However, there are increasing concerns about the environmental impact of salting (TRB, 1992) and sanding, and also their harmful effect on transportation infrastructure. Accordingly, there is great interest in improving the third method, scraping.

Recent studies conducted as part of the Strategic Highway Research Program (SHRP) have shown that the geometry of a blade used on the plow can affect the loads acting on the blade (Nixon 1993, Nixon et al., 1993). The blade variables studied were clearance angle, rake angle, flat width and attack angle, as shown in Figure 1.1. The preliminary experiments (conducted at very low scraping velocities of less than 1.5 ft/s) found that for a clearance angle greater than 2° the forces on the blade were reduced by a

factor of twenty when compared to a blade with a zero degree clearance angle. Further, the scraping forces increased significantly when the blade flat width was more than 3/8 in.

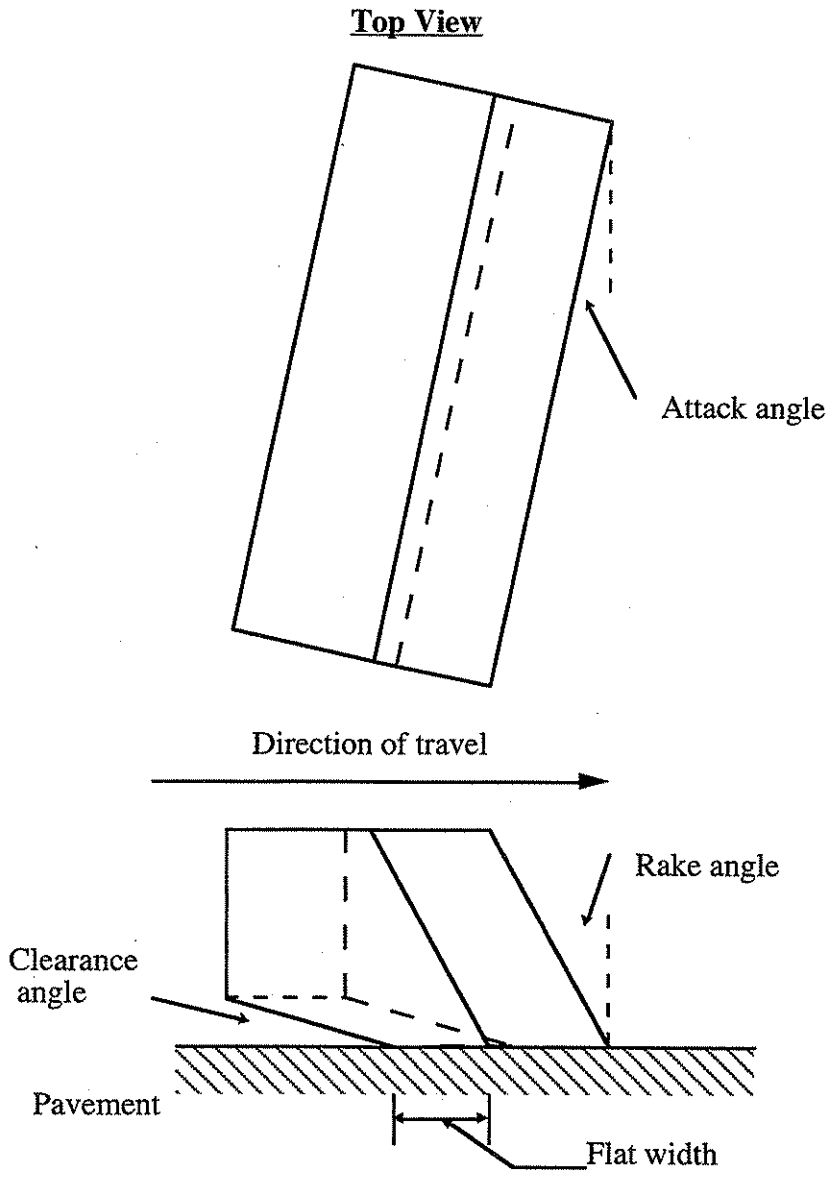

Figure 1.1. Definition of blade geometry variables.

The above studies were extended to higher velocities by means of a custom designed and built ice scraping machine. This second series of tests was conducted at velocities of 5 mph, 10 mph, 15 mph and 20 mph and at temperatures of -5°C and -20°C.

These experiments indicated that a blade with a rake angle of 30°, a clearance angle of 5° and a flat width equal to zero was most efficient for ice removal. It was also concluded from the study that the scraping forces were independent of temperature, and that the scraping resistance decreased with an increase in scraping velocity.

The objective of the project described herein was to conduct further laboratory experiments to determine the blade geometry effects of straight edged and serrated blades for varying ice thicknesses and velocities, and thus to build a more comprehensive understanding of the ice scraping process. The ice scraping machine was first improved, so as to provide more accurate data, by the incorporation of a three axis load cell into the test machine. Straight edged blades with varying blade parameters like rake angle, clearance angle and flat width were tested again and the results compared to previous studies. It was confirmed that blade parameter values of rake angle 30°, clearance angle 5° and zero flat width gave best results. Tests were conducted to compare the performance of straight edged and serrated blades, with both straight edged and serrated blades having the above given blade parameter values.

Chapter 2
Experimental Description

The aim of the experiments was to measure the force required to scrape ice from blocks of concrete, using cutting edges with differing geometry. The primary variables to be studied were the geometry of the cutting edges, the scraping velocity, and the ice layer thickness. By measuring changes in the scraping force as these variables were changed, a model of the ice scraping process could be developed. To simulate field conditions to the best extent possible, the ice samples were grown on specially prepared concrete blocks. The concrete blocks were placed in the ice room to lower their temperature before making the ice samples. The actual scraping process was done using an ice scraping machine. The machine was designed such that a scraping velocity as high as 30 mph could be attained. The loads acting on the blade were measured using a three axis load cell. The scraping velocity was measured using a velocity transducer.

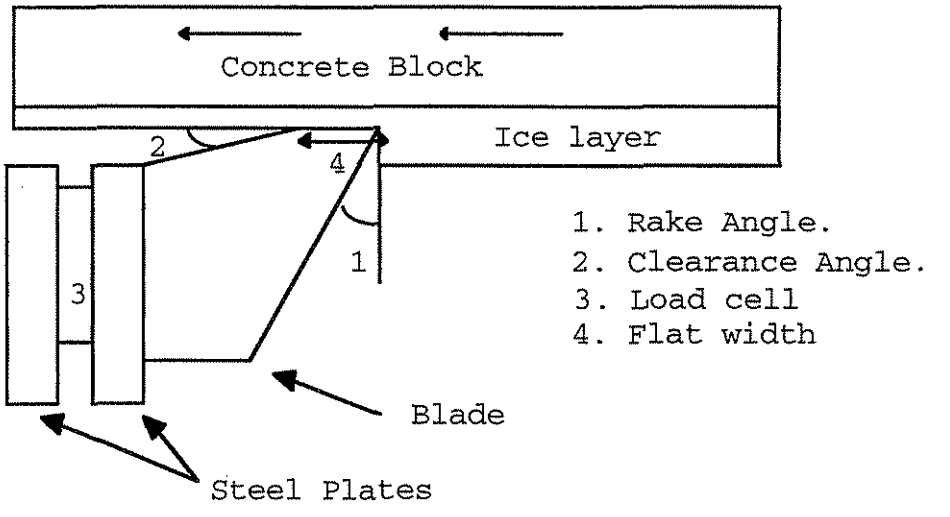

Figure 2.1. The cutting edge striking the ice.

2.1 Experimental Setup

The experimental setup was such that the blade was stationary and the concrete block with the ice sample was in motion. A schematic diagram of the setup is show in Figure 2.1. The blade was fixed to the frame of the ice scraping machine, with the load cell sandwiched (as shown). The concrete block was mounted on a sled attached to a hydraulic ram. It was mounted with the ice layer facing down. The velocity with which the block moved as the blade scraped the ice was monitored.

The setup differs from natural conditions, but is statically and dynamically equivalent to that of a plow scraping an ice layer. The setup makes it easier to record accurately the forces acting on the blade while scraping.

2.1.1 Ice Scraping Machine

The ice scraping machine (Figure 2.2) has a 68 in. long hydraulically propelled piston or ram. The ram is mounted on a W 10x49 structural beam, which provides stiffness and structural support. The hydraulic system is designed to operate under a pressure of 3000 psi, produced by a differential displacement pump.

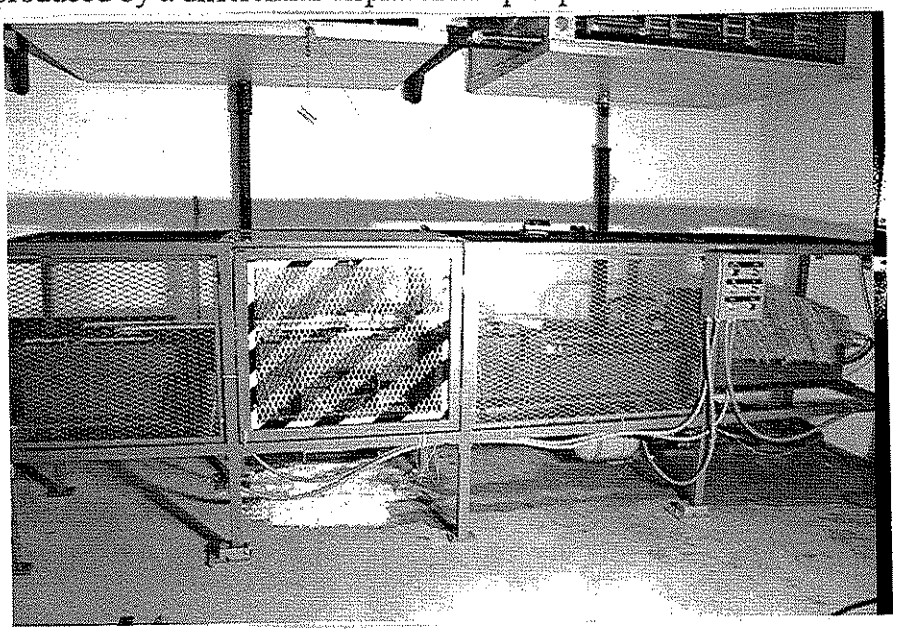

Figure 2.2 The ice scraping machine.

The concrete block (Figure 2.3) is mounted on a sled connected to the end of the ram. The first 16 in. of the stroke allows the concrete block to accelerate to the required velocity. The ice on the block then hits the blade and the ice scraping action occurs. The off switches trigger immediately after the scraping and the block comes to a stop in the remaining distance. The concrete block is 12 in. x 4 in. x 4 in. in size. A shock absorber

has been mounted at the end of the stroke as a safety precaution. A choke control selector valve controls all operations.

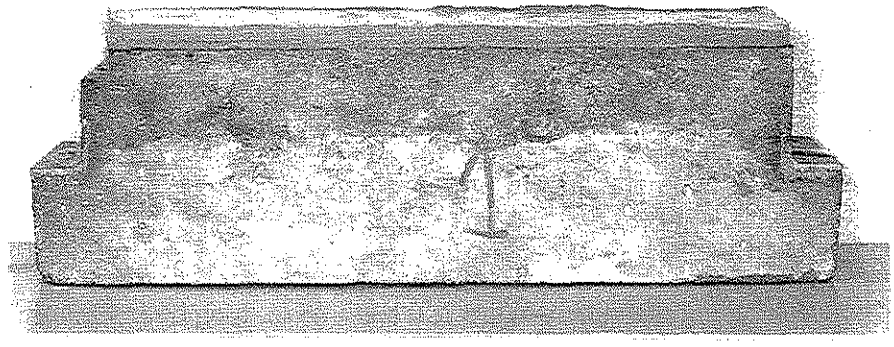

Figure 2.3 The concrete block

The selector valve has three control positions; one for forward movement, one for backward and the third for neutral position of operation. A four gallon accumulator, placed in the flow line between the pump and the selector valve, operates at an internal pressure of 1500 psi, thus ensuring the transfer of large quantities of fluid while operating at high velocities. Once the scraping is over, the selector valve switches to a neutral position, shutting off all fluid flow. While the sled is still in motion, with significant momentum, the pressure upstream of the piston rises considerably whereas the pressure downstream of the piston decreases. This process creates a decelerating effect.

A 2000 psi, relief valve accounts for this differential pressure. If the fluid pressure in the line rises above 2000 psi, the valve opens allowing the fluid to flow back to the other side of the piston. During deceleration a negative pressure can build up since the flow is shut off and the piston is still in motion. A one half gallon accumulator placed downstream of the choke control valve, just before of the hydraulic piston, serves as an additional reservoir of fluid and hence prevents negative pressure.

2.1.2 Load Cell Calibration

The impact forces on the blade while scraping the ice were measured by a three axis load cell. The load cell was held tightly between the machine frame and the blade. The

operation of the load cell was based on the piezoelectric properties of quartz. When a strain is applied to the load cell, the electrical properties of the quartz change in proportion to the strain. To keep the strain proportional to the stress the load cell has to be prestressed. The prestressing was done using a torque wrench. About 22,000 lbs. of prestressed force was applied for the testing. Since the measured forces were much lower than the prestressed force, no slip occurred. The load cell was calibrated before any testing took place.

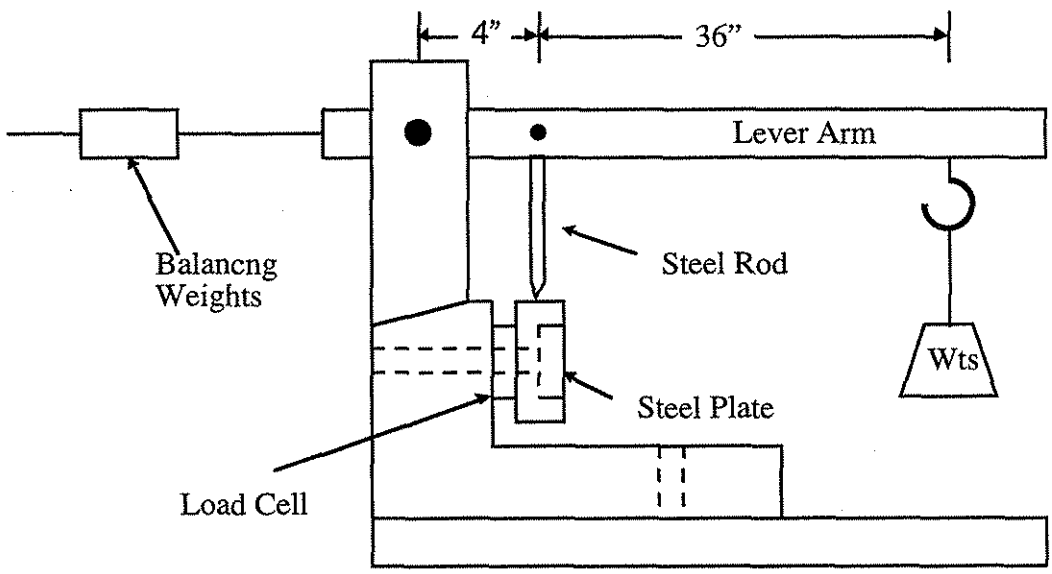

Figure 2.4. Load cell calibration setup for x and y directions.

The load cell was calibrated in three orthogonal directions (x, y, and z). The calibration system is shown in Figures 2.4 and 2.5. The vertical arm has a cantilever arm attached to it. The cantilever arm was balanced by weights such that it was in a horizontal position. The load cell could be mounted on the horizontal or vertical arm depending which axis was being calibrated. The cell was mounted on horizontal arm for calibrating the cell in the z-direction. For calibrating in the x and y directions, it was mounted on the vertical arm (Figure 2.4). The cantilever arm has a steel rod that rests lightly on the load cell. The dimensions of the arm were such that if weights were hung at the free end of the cantilever, ten times the weight acted on the load cell through the steel rod. A voltmeter was connected to the load transducers and the change in voltage with change in load on the cell was recorded. The calibration curves were obtained by placing a curve-fit through the data points.

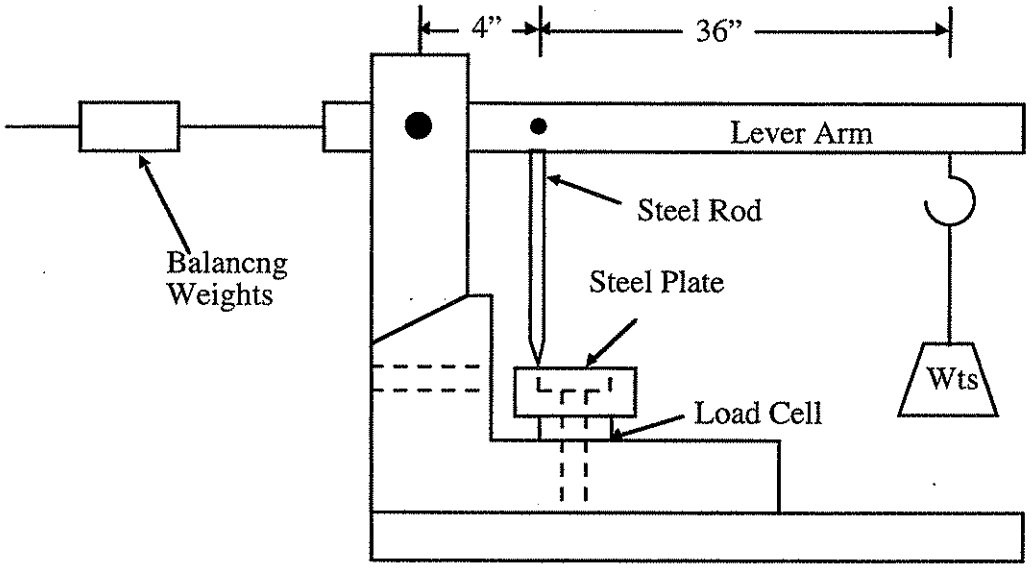

Figure 2.5. Load cell calibration setup for z direction.

2.1.3 Velocity Transducer Calibration

A Linear Voltage Displacement Transformer (LVDT) was used for position measurement. For the purpose of calibration, the sled was disconnected from the piston, and moved manually. For different positions of the sled the voltage was recorded using a voltmeter. The plot between position and voltage was obtained and the curve was highly linear. The relationship between position and voltage was used to determine the scraping velocity.

2.1.4 Design and Manufacture of the Concrete Samples

The ice samples for testing were grown on specially designed concrete blocks. The concrete blocks were made with a C4 concrete mix. Each block was 12 in. x 4 in. x 4 in. in size. The blocks were cast such that the sides made an angle of 2° with respect to the vertical. The top surface of the concrete block was roughened with a brush while the concrete was still viscous. The sled carrying the concrete block for testing was made such that the block fit into it exactly on three sides, with some gap between the block and the sled on the fourth side. To avoid even a small displacement of the block due to the impact of the blade on the ice, the concrete block was prestressed using a steel bolt. A steel plate pressing against the concrete block, with a fastening bolt between the plate and the sled were provided such that, on tightening the bolt a compression force was exerted on the concrete block by the steel plate.

The ice on the concrete blocks was grown in layers. This avoided the formation of air pockets within the ice during ice formation. The air pockets cause additional areas of stress concentration which do not exist in nature. Each layer of water, around 1/8 in. in thickness was allowed to freeze before the next was added and the number of layers depended on the final thickness of ice required. The water was held in place on the block by a foam strip wound tightly round the concrete block (Figure 2.6). The temperature in the ice room was controlled by a thermostat and was maintained at 21°F with an accuracy of ±2°F.

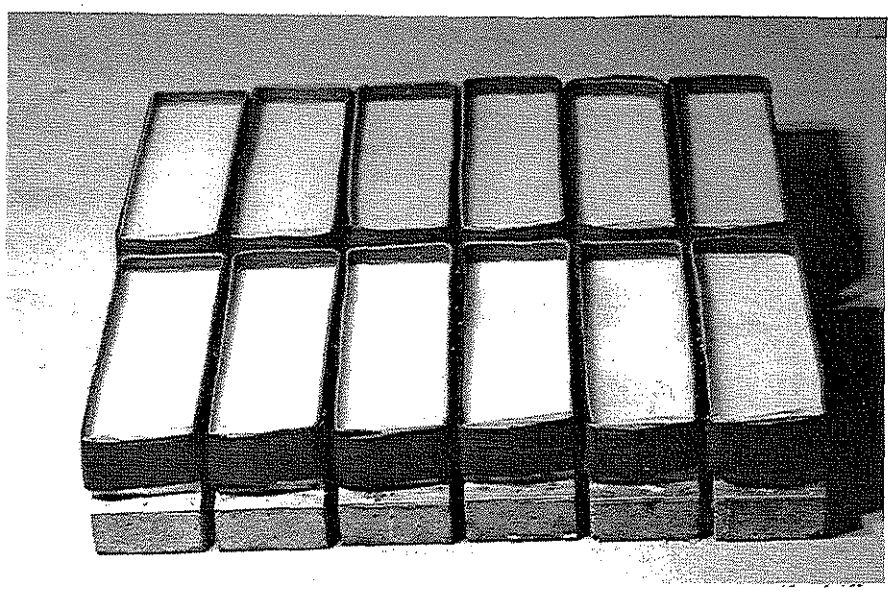

Figure 2.6 Foam strips acting as dams

2.2 Parameters and Variables

The blade parameters for the classical or straight edged blades (see Figure 2.7) were

1) Rake angle (0°, 15°, 30° and 45°)

2) Clearance angle (2°, 5° and 10°) and

3) Flat width (0 in., 1/8 in. 1/4 in and 5/8 in.)

4) Edge effect.

Based on the results obtained for straight edged blades, all blades used for further testing had standard parameters of rake angle 30°, clearance angle 5° and flat width 0 in.

Tests were also conducted with these parameters to determine the ice thickness effect and scraping velocity effect on scraping forces.

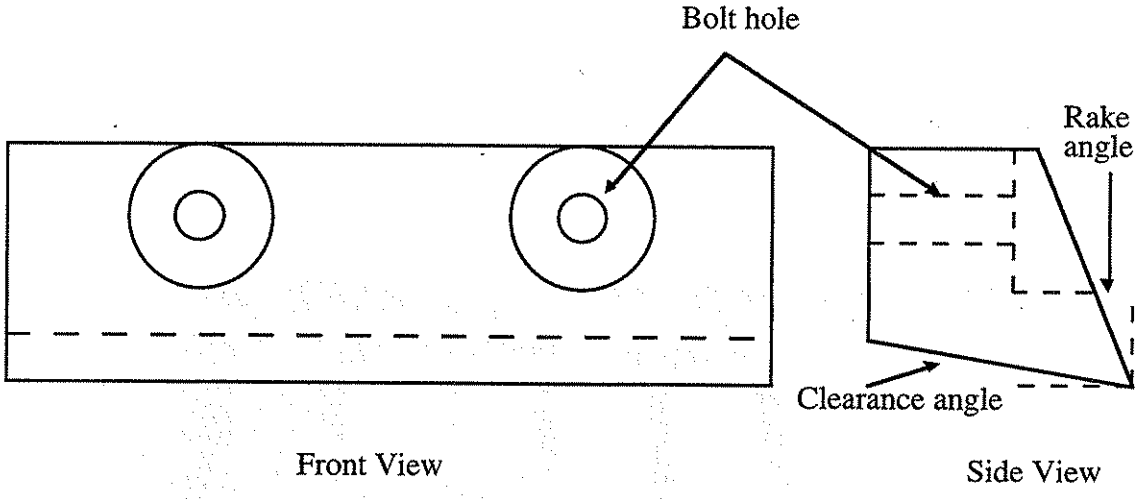

Figure 2.7. Cutting edge geometry of a classical blade.

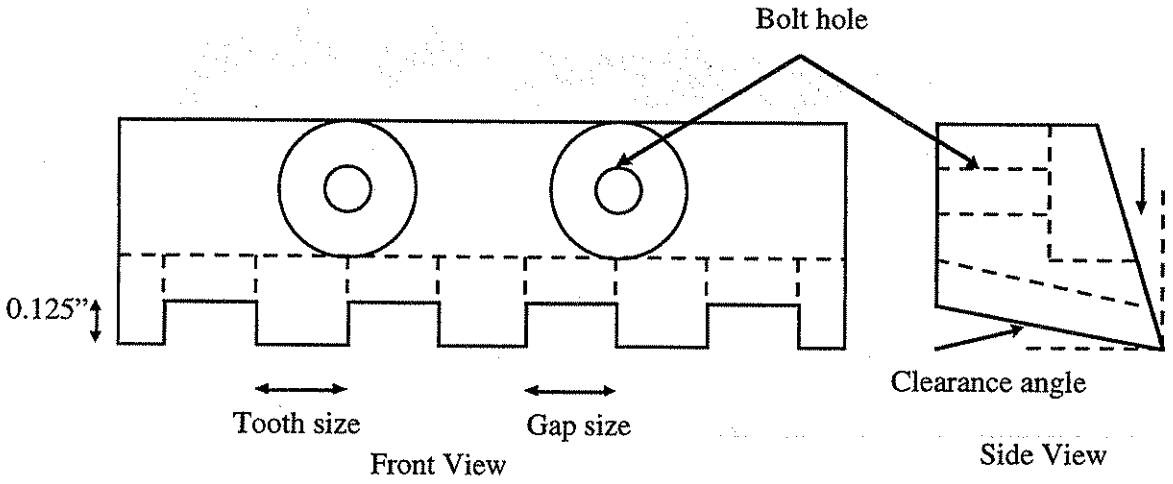

Figure 2.8 Cutting edge geometry with rectangular serration.

2.3 Typical Procedure

The concrete blocks on which the ice layers were formed were always kept in the ice room, so that when the samples were to be made, the temperature of the blocks was below freezing. Prior to making the samples, water (ordinary tap water) was taken in a large container and placed in the ice room for about 30 to 40 minutes, to cool it and bring

the temperature close to the freezing point. This process prevented the formation of air bubbles in the samples. While the water was cooling, the foam strips were wrapped tightly round the concrete blocks so that water could be retained on top of the blocks. A small quantity of grease was applied to the sides of the concrete blocks before wrapping the foam, to avoid leakage of water.

When the water became sufficiently cold, it was poured carefully on top of the concrete blocks, the layer of water not exceeding 0.125 in. The second layer was not applied until the first layer of water was completely frozen. On average each layer took about 1 to 1.5 hr. to freeze. The samples were usually prepared in the morning and the tests conducted at the end of the day.

The ice scraping machine was switched on at least ten minutes before the actual testing was done. In order to ensure the oil in the hydraulic pump was adequately warmed up, the sled was made to run forwards and backwards several times, taking care to start at very low velocities and then slowly increasing until the test velocity was attained smoothly. This caused the hydraulic oil to flow and warm up

Testing was conducted in batches. For each batch, 12 samples were prepared and the concrete blocks numbered. In order to determine the efficiency (defined as the percentage of ice removed by volume) of each run, the weight of ice scraped off each block during scraping was required. Once the sample was prepared and ready for testing, the foam strip was removed and the thickness of the ice layer formed was measured using a scale. The concrete block was placed in the sled with the ice layer facing downwards, and the prestressing bolt was tightened with a wrench so that the concrete block did not move. Before running the test, the data acquisition system was started on the computer. The switch to move the sled forward was turned on and the run completed. The same process was repeated for the other samples in the batch. After each batch of testing was complete, the concrete samples were cleaned off and made ready for the next batch of testing.

2.4 Data Acquisition and Data Handling

Data acquisition and handling was done using a PC and the software, LABTECH NOTEBOOK. The variation of voltages, with the variation of loads in the three directions on the load cell and with the displacement of the sled, as transmitted by the load cell transducers and velocity transducer through independent channels, were recorded by the computer. The frequency and the time interval for data acquisition could be set as required. A visual plot of the four voltages corresponding to the three loads and the displacement

with respect to time, was shown on the computer during the scraping process. The data acquired for each test run were stored in separate files.

Before each test run the initial values of the voltages were recorded and stored from all four channels. After the test run when the final values were acquired, the average of the initial values were subtracted from the final values to give the actual voltages corresponding to the loads. The voltages were then converted to their corresponding loads or displacement as the case may be using the calibration curves.

Chapter 3
Experimental Results

3.1 Introduction

The averaged results of the ice scraping tests for selected runs are presented in this chapter. The type of output obtained from each experiment varies significantly between each run. The magnitude of forces and type of output changes with varying blade parameters. All experimental results obtained for this study contain scattered data. However, the difficulty of analysis was not only due to the spread of data, but also to ice chipping. This chipping resulted in a sudden drop of forces and therefore effected the final average. The complete table of results is located in Appendix A. When dealing with results of this type, it is difficult to adequately represent the experimental output with a single number or even an average value for a each experiment. In order to obtain comparable and reasonable results for analysis, a large number of experiments were necessary.

There were three sets of parameters that were considered in this study:

1. Blade variables
2. Thickness of scraped ice
3. Scraping velocity

The results of the scraping tests according to these three sets of variables are presented in the following sections.

3.2 Blade Variables

The blade variables referred to in this section are shown in Figure 1.1

3.2.1 Rake Angle Effect

Blades with rake angles of 0° ,15°, 30° and 45° were tested at varying velocities. Even though the load cell was capable of measuring forces in three directions, only

horizontal and vertical forces were of analytical significance. For each run an average force was calculated for both horizontal and vertical directions. Because of the large scatter of results and because of variation between tests (for the same blade with common velocity and thickness), an average of several individual runs was taken. Data for rake angles, 0°, 15°, 30°, and 45° are plotted in Figures 3.1 and 3.2.

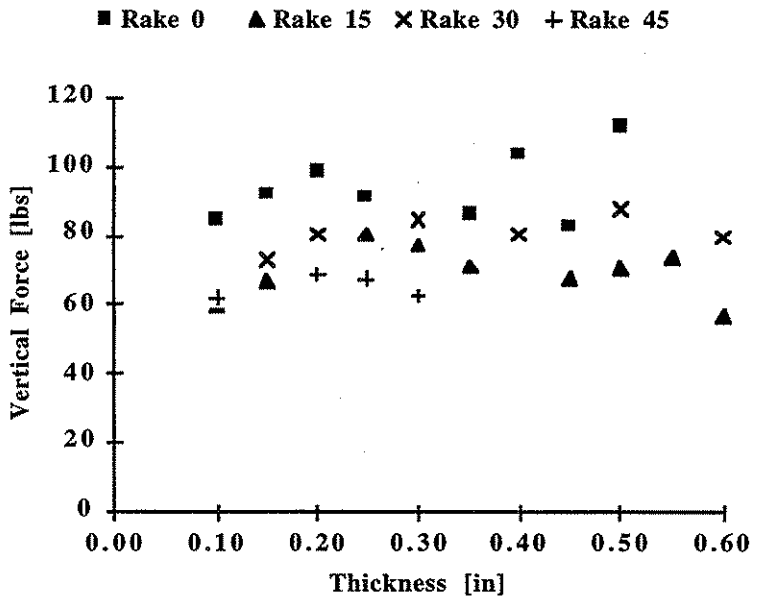

Figure 3.1 Average vertical force vs. thickness for various rake angles (Vel=10 ft/s)

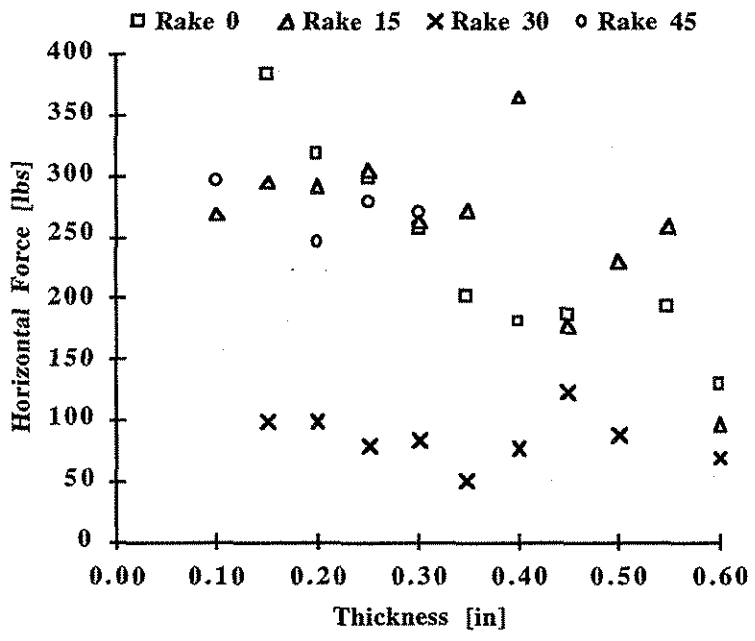

Figure 3.2 Average horizontal force vs. thickness for various rake angles (Vel=10 ft/s)

3.2.2 Clearance Angle Effect

The clearance angle effect was tested for three different values at 2°, 5°, and 10°. The average vertical and horizontal forces are plotted in Figures 3.3 and 3.4 respectively. Rake angle 30° and zero flat width were constant for all three blades.

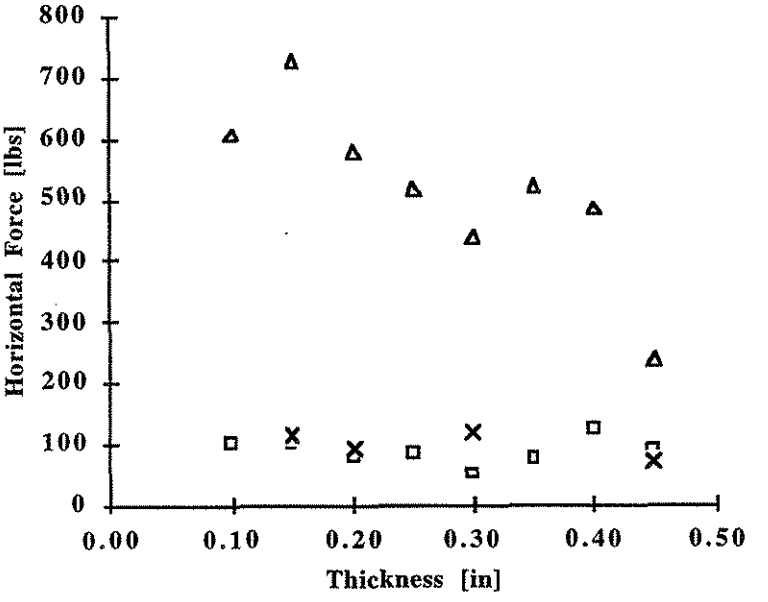

Figure 3.3 Average vertical force vs. thickness for various clearance angles (Vel=9 ft/s). The clearance angles are 2° (Δ), 5° (□), and 10° (×)

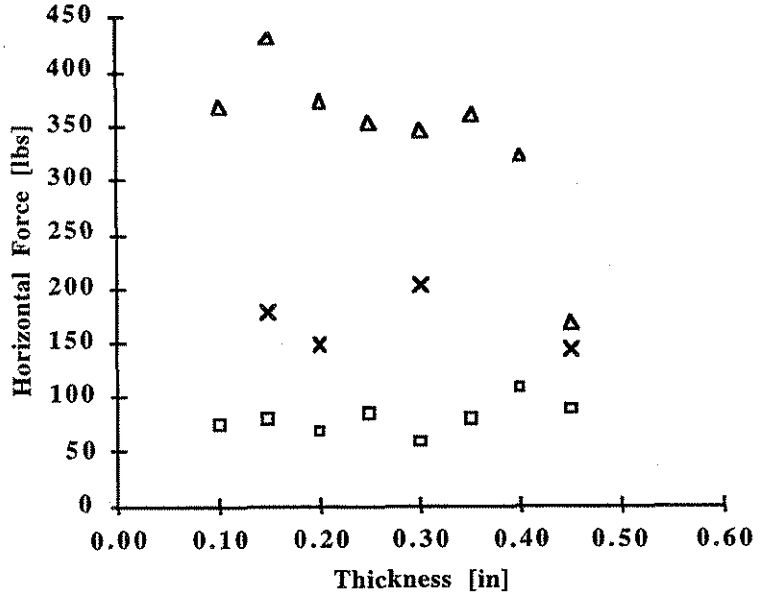

Figure 3.4 Averaged results horizontal force vs. thickness for various clearance angles (Vel=9 ft/s). The clearance angles are 2° (Δ), 5° (□), and 10° (×)

3.2.3 Flat Width Effect

Due to blade wear, it was important for the study to analyze the flat width effect on the scraping forces. Four different blades with varying flat widths were tested. For this analysis, blade rake angle and clearance angle were constant at 30° and 5° respectively. The results are presented Figures 3.5 and 3.6.

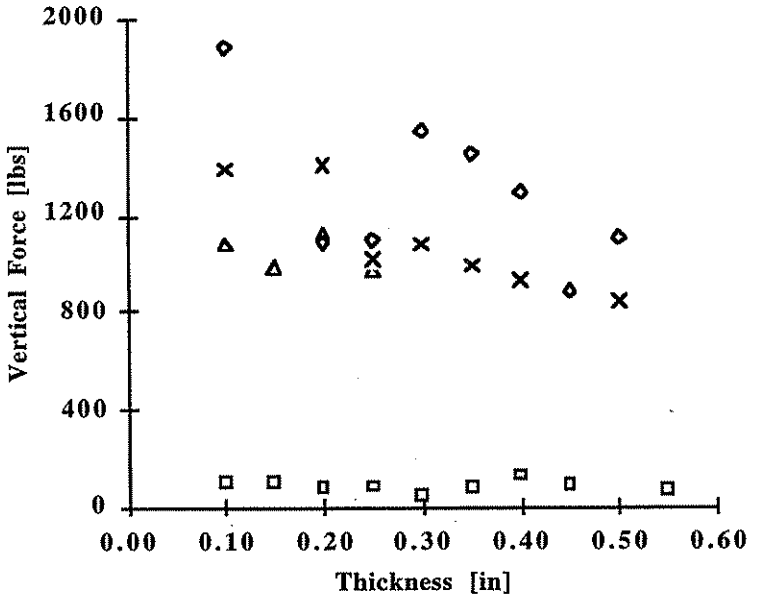

Figure 3.5 Average vertical force vs. thickness for various flat widths. The flat widths are 0 in. (□), 0.125 in. (Δ), 0.3 in.(×), and 0.4 in. (◊).

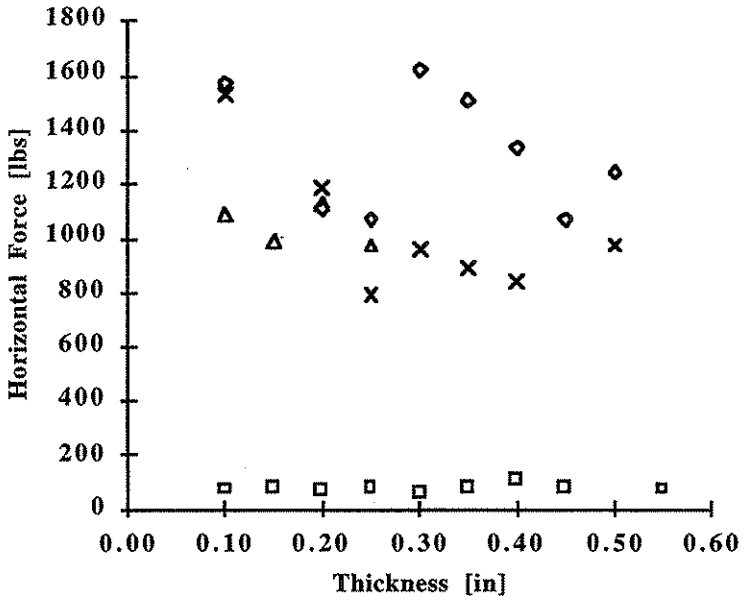

Figure 3.6 Average horizontal force vs. thickness for various flat widths. The flat widths are 0 in. (□), 0.125 in. (Δ), 0.3 in.(×), and 0.4 in. (◊).

3.2.4 Blade Edge Effect

The samples on which ice was grown were 4 in. in width, however, the blades were manufactured at 5 in.. Therefore, all ice was removed from the concrete block. It was of interest to test a blade of smaller width than that of the concrete block, in this case with a blade width of 3.2 in. These results are presented Figures 3.7 and 3.8. The results are given in pounds per inch of scraped area.

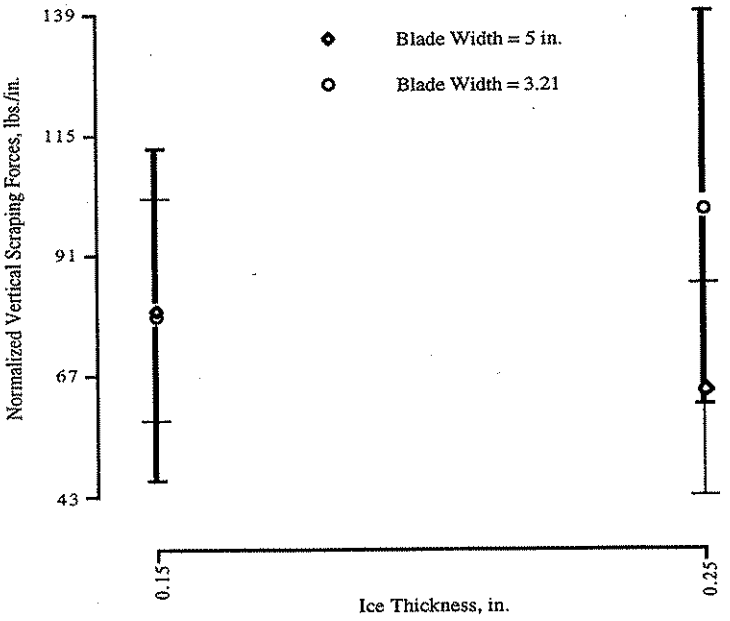

Figure 3.7 Average vertical force vs. thickness for blades with various widths

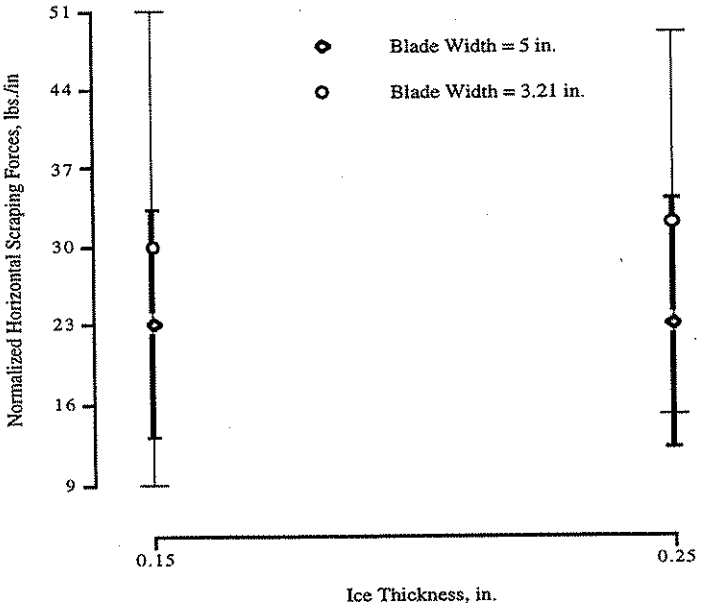

Figure 3.8 Average horizontal force vs. thickness for blades with various widths

3.2.5 Serrated Blades

In previous studies, results showed that ice failed in chips or flakes of various sizes. Because of this reason, it was believed that ice could be removed effectively using

various designs of serrated blades. The following sections present results of serrated blades with square teeth of different sizes.

Figures 3.9 and 3.10 give visual representation of the average forces in the horizontal and vertical directions. All figures in this section contain results only for velocity of 10 ft/s. Data obtained for other velocities are available in the Appendix A.

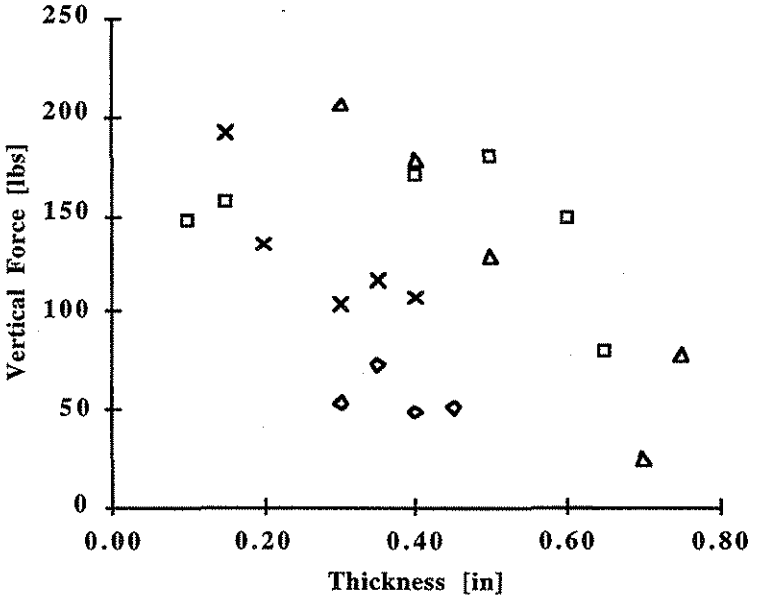

Figure 3.9 Average vertical forces vs. thickness for serrated blades for various teeth sizes. The sizes of the teeth are 0.125 in. (□), 0.25 in. (Δ), 0.5 in. (×), and 1.0 in. (◊).

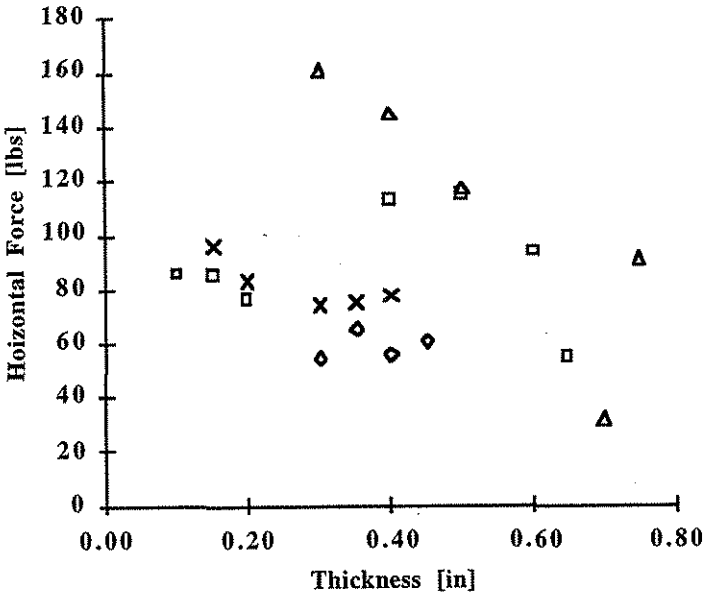

Figure 3.10 Average horizontal forces vs. thickness for serrated blades for various teeth sizes. The sizes of the teeth are 0.125 in. (□), 0.25 in. (Δ), 0.5 in. (×), and 1.0 in. (◊).

3.2 Ice Thickness Effect

Five blades were chosen to test the effect of ice thickness on scraping forces. Figures 3.11 through 3.20 present the results of a blade with rake angle 30°, clearance angle 5°, and a zero flat width. Four of the five blades were serrated blades of 0.125, 0.25, 0.5, and 1 in. square teeth.

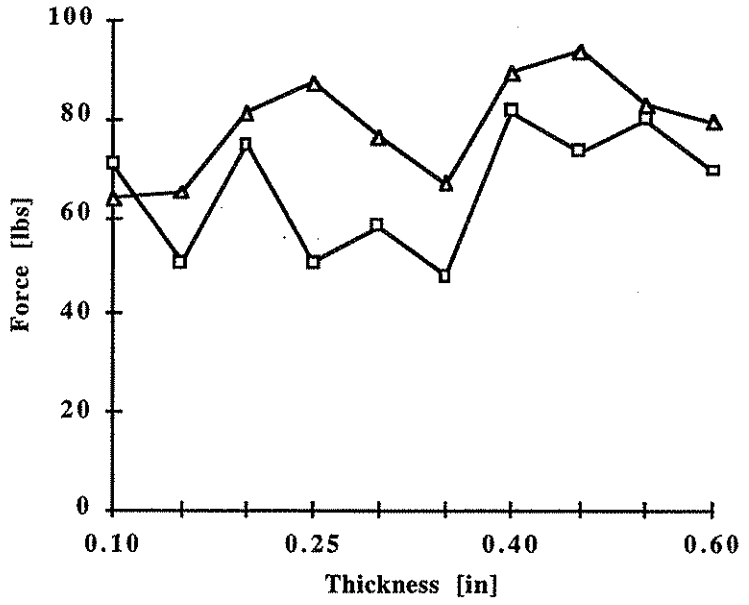

Figure 3.11 Average forces vs. ice thickness for blade with a rake angle of 30°, clearance angle of 5°, and zero flat width. The horizontal force is denoted by (□) and the vertical force is denoted by (Δ)

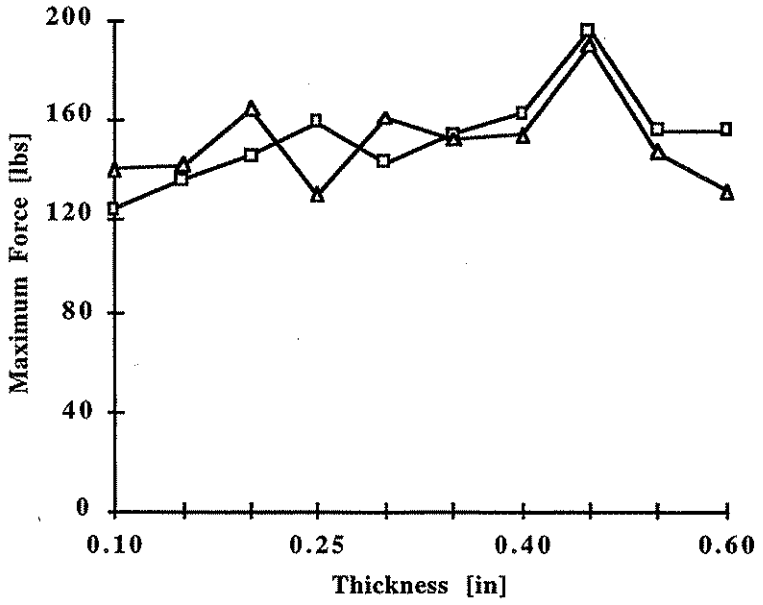

Figure 3.12 Maximum forces vs. ice thickness for blade with a rake angle of 30°, clearance angle of 5°, and zero flat width. The horizontal force is denoted by (□) and the vertical force is denoted by (Δ)

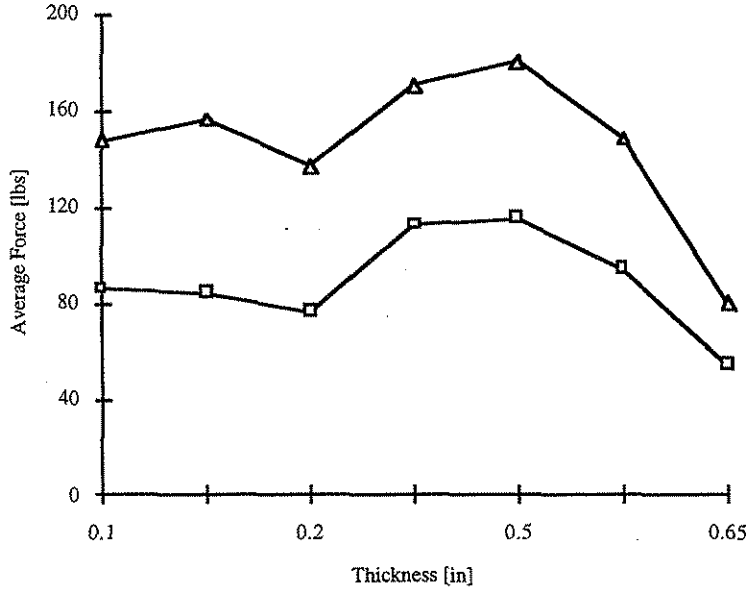

Figure 3.13 Average forces vs. ice thickness for blade with a rake angle of 30°, clearance angle of 5°, and tooth size of 0.125 in. The horizontal force is denoted by (□) and the vertical force is denoted by (Δ)

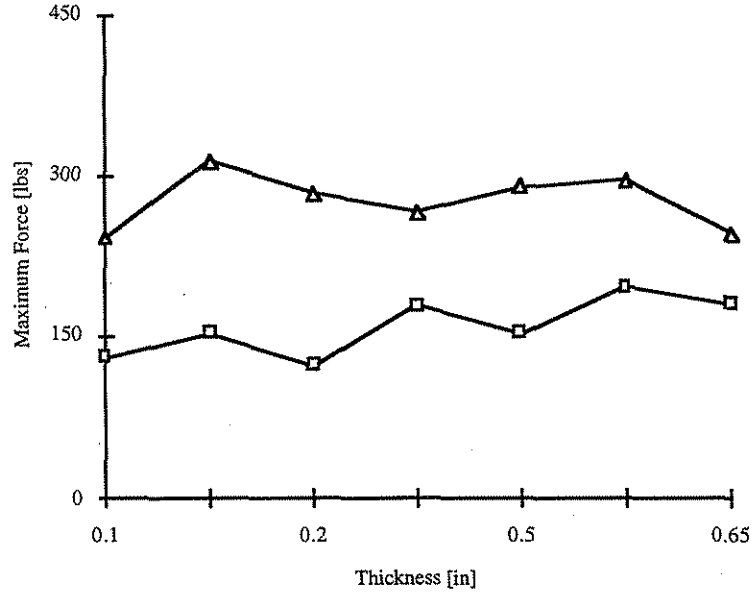

Figure 3.14 Maximum forces vs. ice thickness for blade with a rake angle of 30°, clearance angle of 5°, and tooth size of 0.125 in. The horizontal force is denoted by (□) and the vertical force is denoted by (Δ)

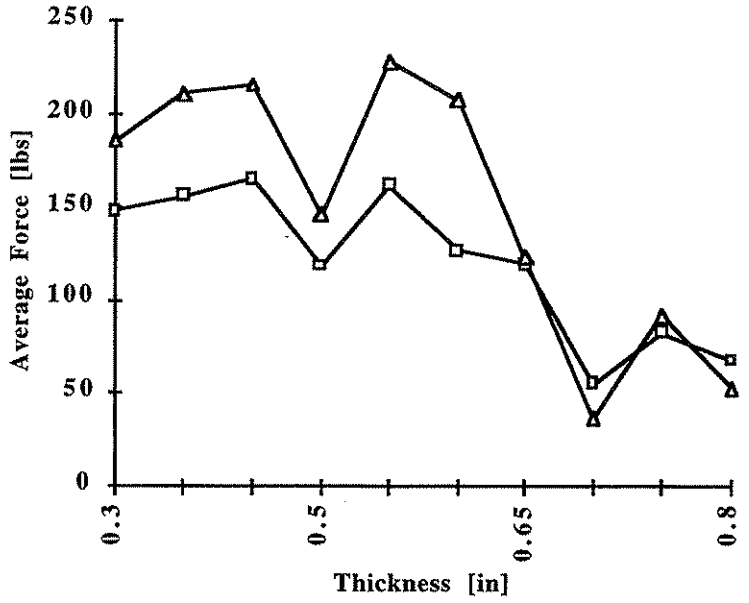

Figure 3.15 Average forces vs. ice thickness for blade with a rake angle of 30°, clearance angle of 5°, and tooth size of 0.25 in. The horizontal force is denoted by (□) and the vertical force is denoted by (Δ)

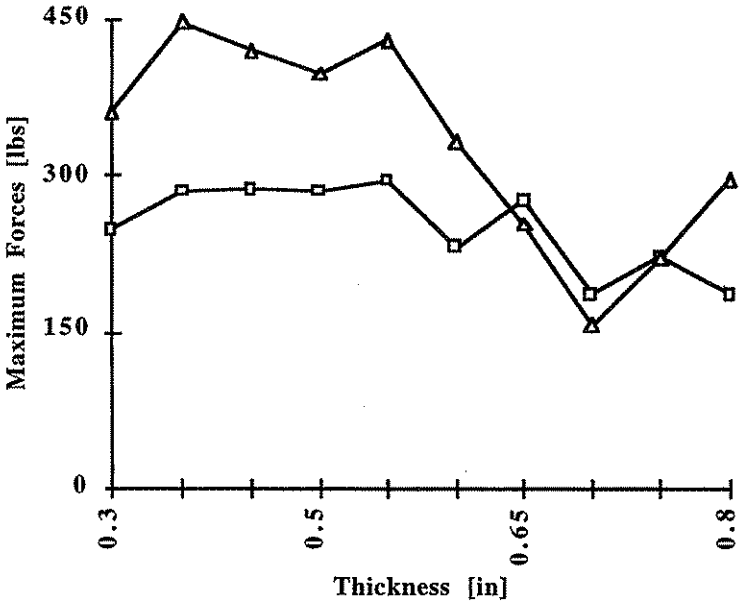

Figure 3.16 Maximum forces vs. ice thickness for blade with a rake angle of 30°, clearance angle of 5°, and tooth size of 0.25 in. The horizontal force is denoted by (□) and the vertical force is denoted by (Δ)

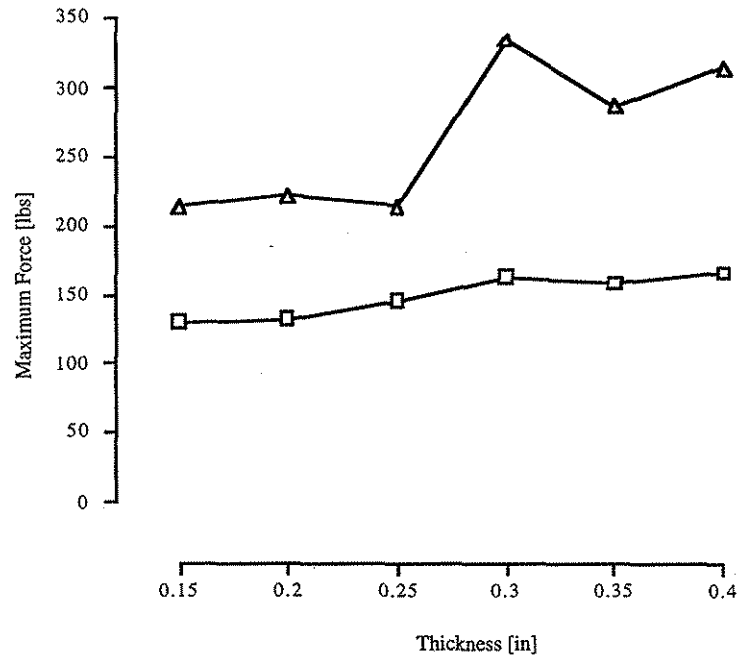

Figure 3.17 Maximum forces vs. ice thickness for blade with a rake angle of 30°, clearance angle of 5°, and tooth size of 0.5 in. The horizontal force is denoted by (□) and the vertical force is denoted by (Δ)

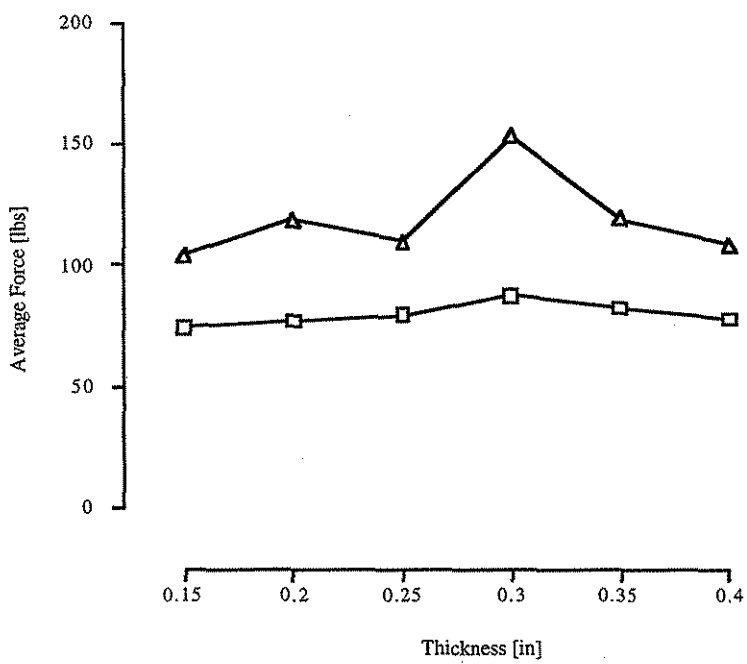

Figure 3.18 Average forces vs. ice thickness for blade with a rake angle of 30°, clearance angle of 5°, and tooth size of 0.5 in. The horizontal force is denoted by (□) and the vertical force is denoted by (Δ)

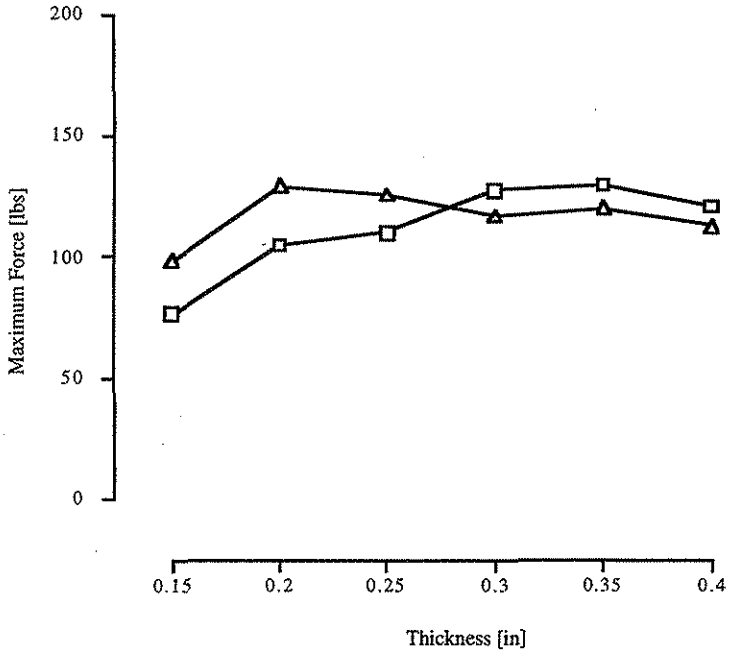

Figure 3.19 Maximum forces vs. ice thickness for blade with a rake angle of 30°, clearance angle of 5°, and tooth size of 1 in. The horizontal force is denoted by (□) and the vertical force is denoted by (Δ)

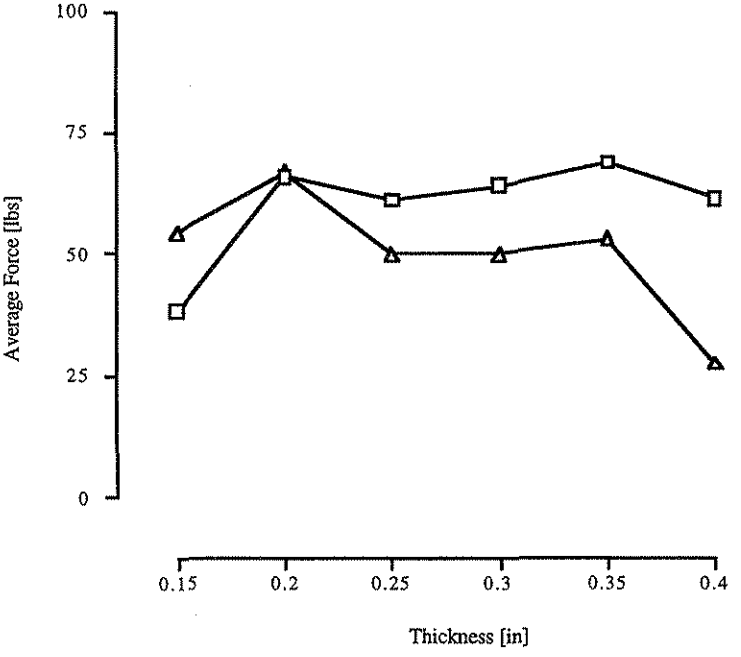

Figure 3.20 Average forces vs. ice thickness for blade with a rake angle of 30°, clearance angle of 5°, and tooth size of 1 in. The horizontal force is denoted by (□) and the vertical force is denoted by (Δ)

3.4 Velocity Effect

In the process of removing ice from roads using cutting edges, velocity may have an effect on scraping forces. Figures 3.21 through 3.24 represent the relationship both vertical and horizontal scraping forces for a constant ice thickness of 0.3 in., for two blades: one without serrations, the other with teeth 0.25 in. wide with equal sized gaps between the teeth..

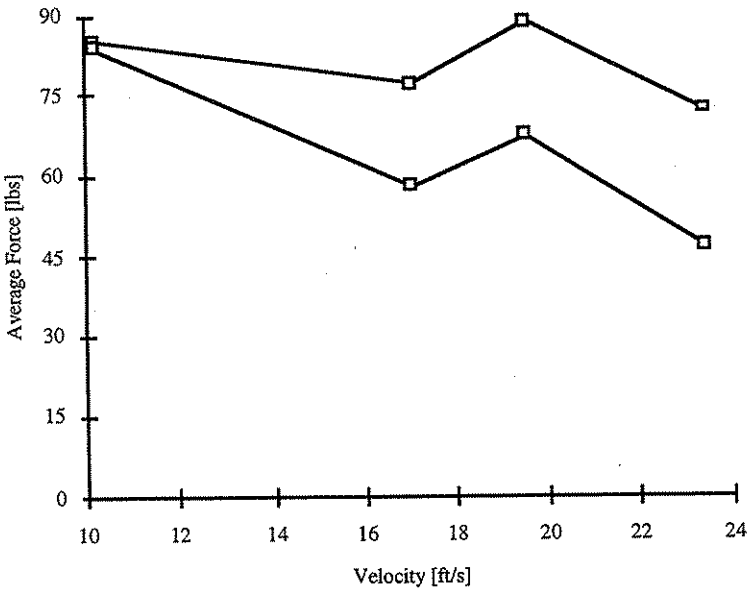

Figure 3.21 Average forces vs. thickness for blade with a rake angle of 30°, clearance angle of 5°, and zero flat width. The horizontal force is denoted by (□) and the vertical force is denoted by (Δ)

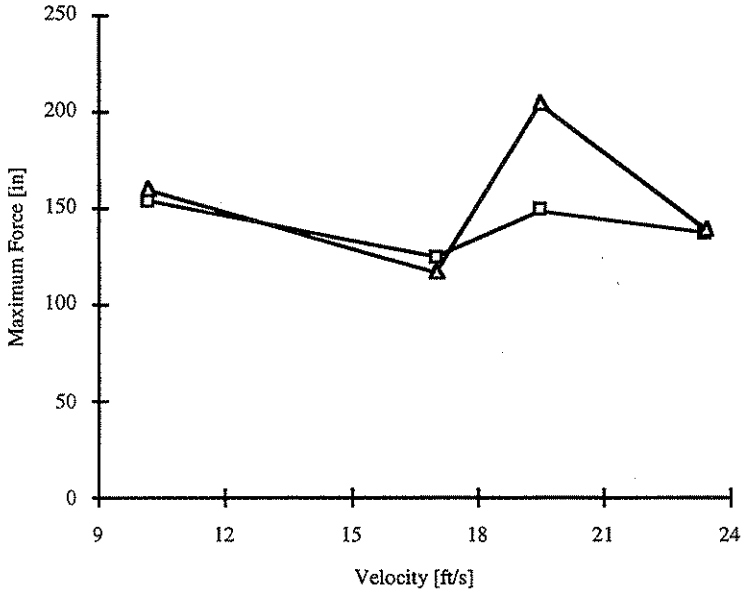

Figure 3.22 Maximum forces vs. thickness for blade with a rake angle of 30°, clearance angle of 5°, and zero flat width. The horizontal force is denoted by (□) and the vertical force is denoted by (Δ)

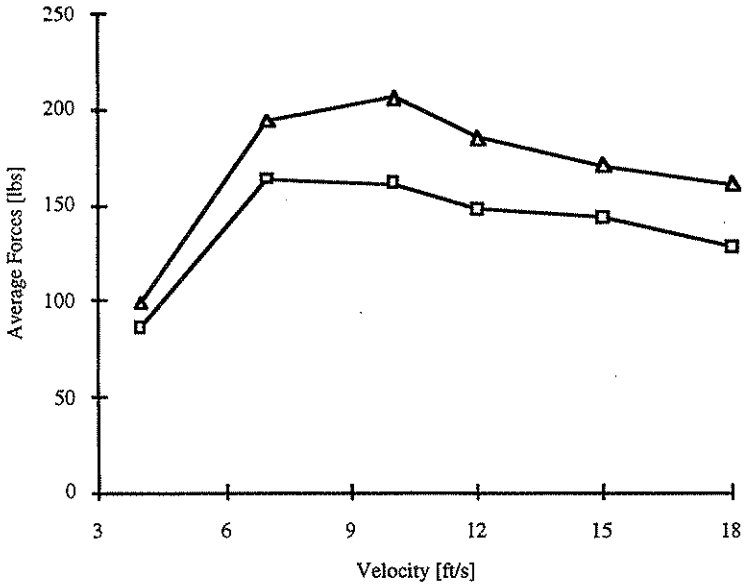

Figure 3.23 Average forces vs. thickness for blade with a rake angle of 30°, clearance angle of 5°, and tooth size of 0.25 in. The horizontal force is denoted by (□) and the vertical force is denoted by (Δ)

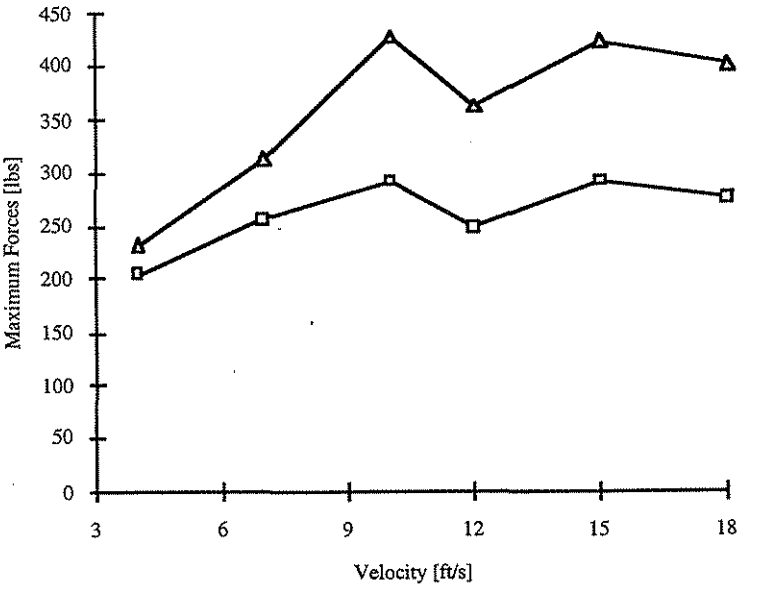

Figure 3.24 Maximum forces vs. thickness for blade with a rake angle of 30°, clearance angle of 5°, and tooth size of 0.25 in. The horizontal force is denoted by (□) and the vertical force is denoted by (Δ)

Chapter 4
Discussion

4.1 Introduction

This study has two aims: to determine the process by which ice is scraped from the road; and to determine whether serrated blades offer any benefits for ice scraping. In this chapter the results presented in Chapter 3 are discussed with these two aims in mind.

4.2 Rake Angle Effect

Four different rake angles were analyzed: 0°, 15°, 30°, and 45°. As shown in Figure 3.2, a rake angle of 30° has been shown to produce the best results with respect to vertical force. It can be seen that for small thicknesses (about 0.1 in.), the difference in the magnitude of forces for rake angle 30° versus the other three rake angles is approximately 200 lbs. However, as the scraping thickness increases (up to 0.6 in.), this difference becomes smaller (about 20-50 lbs).

The horizontal force reactions versus thickness for each rake angle are shown in Figure 3.1. The magnitudes of these forces are much smaller than the vertical forces. Also, horizontal force decreases with increasing rake angle. These results are consistent considering that an angled blade would reduce the amount of energy transferred to the broken ice chips. However a "blunt" blade would redirect the ice chips in the opposite direction thus supplying them with more energy. This phenomenon is illustrated in Figure 4.1.

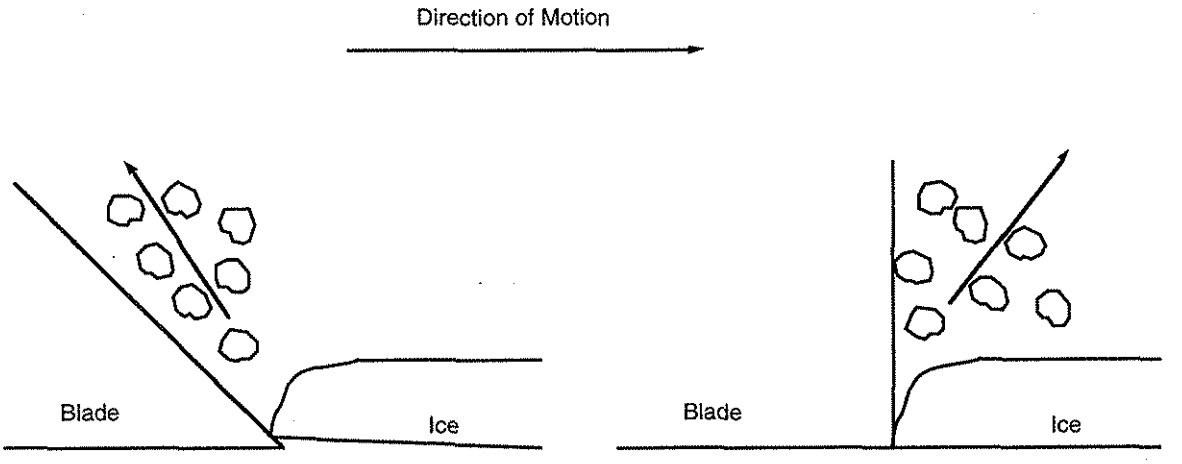

Figure 4.1 Direction of ice chips for blunt and angled blades

4.3 Clearance Angle Effect

Another variable that was taken into consideration was clearance angle. Blades with three clearance angles, 2°, 5°, and 10°, with flat widths of zero were tested. Figure 3.3 shows that clearance angles of 5° and 10° give approximately the same vertical forces for varying thicknesses. Blades with clearance angle 2° had a much higher vertical reaction force. As was observed before, the difference in these forces decreases as the thickness of scraped ice increases. The results collected for horizontal force were much lower for the blade with clearance angle 5° which would indicate that this angle is the most desirable one. The clearance angle effect sheds particular light on the ice scraping process. It appears that as the blade interacts with the ice, ice ahead of the blade is fragmented. This fragmentation occurs both above and below the horizontal plane along which the tip of the cutting edge moves. While the ice above this plane is ejected in front of the blade, the ice fragments beneath the cutting tip plane must pass beneath the cutting edge. For this to occur, the ice fragments must be compressed, which requires work to be done. The degree of compression will be greater for a smaller clearance angle (below some value) and also greater for a greater flat width. This description of the ice-scraping process is confirmed both by the observed clearance angle and flat width effects, and by observed ejection of ice fragments from behind the cutting edge, as documented in the field experiments of Nixon and Frisbie (1993).

4.4 Flat Width Effect

In real life application, plow blades are subject to wear which increases the flat width of the blade. For practical application, it was important during this study to determine the effect of flat width on the efficiency of scraping and the resulting forces. By studying the various flat widths of blades, it was determined that with increasing flat widths there was a large increase in both vertical and horizontal forces. Figures 3.5 and 3.6 show that a flat width of 0.125 in. increases the reaction forces by magnitudes of 10 for the vertical force and 4 for the horizontal force. These results indicate a tremendous blade wear effect on scraping forces.

4.5 Edge Effect

Another aspect considered in this study was blade edge effect. For all previous tests, the blade width was 5 in. (larger than the width of the concrete sample) and, as a result, all ice was removed from the concrete block. To test edge effect, a blade of 3.2 in. width was used. Figures 3.7 and 3.8 show the data obtained from both the 5 inch and 3.2 inch blades. In order to show edge effect, the reaction forces were divided by the width of the blade. It can be seen that for various thicknesses, the smaller blade (3.2 in.) produced higher reaction forces. This may reflect the complex stress state at the edge of the smaller blade as it cuts a groove in the ice.

4.6 Serrated Blades

It should be noted at this point, that because the blade with rake angle 30°, clearance angle 5°, and flat width zero showed the best results, all the serrated blades were made with these parameters. For all blades, the teeth sizes and the spacing between them were kept at a ratio of one. The teeth were a quarter inch deep. Blades with four different tooth sizes (0.125 in., 0.25 in., 0.5 in., and 1.0 in.) were tested. These blades leave a grooved surface, each groove corresponding to a different tooth size. The blade with a tooth size of 1.0 inch had the smallest reaction forces. This blade, however, did not remove ice efficiently. As the width of tooth size decreased, the height of the grooves also decreased (as illustrated in Figures 4.2 and 4.3).

Both vertical and horizontal forces increased for blades of smaller tooth sizes (0.25 in. and 0.125 in.). Because of their tooth sizes, these blades were able to remove a larger volume of ice. The serrated blades of smaller teeth sizes exerted smaller reaction forces than an un-serrated blade with rake angle 30° and clearance angle 5°.

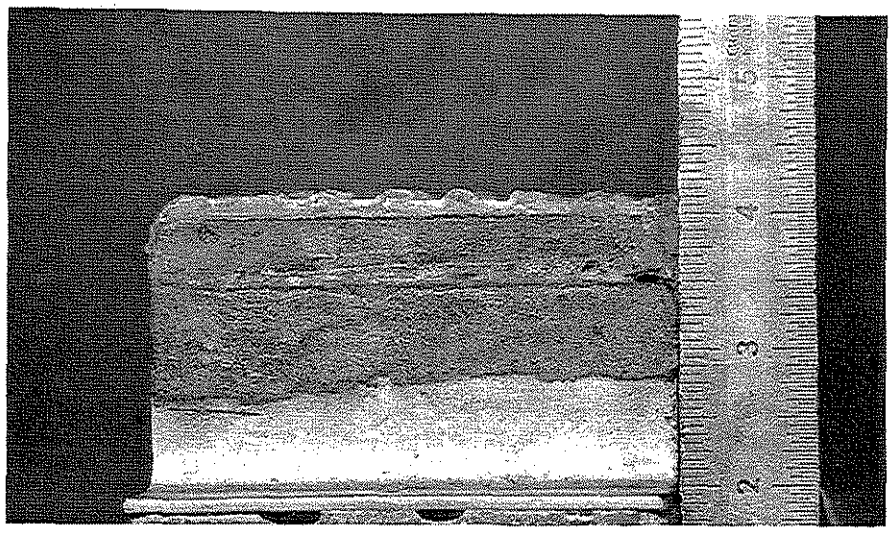

Figure 4.2 Side view of a serrated blade (0.25 in.) surface after a run

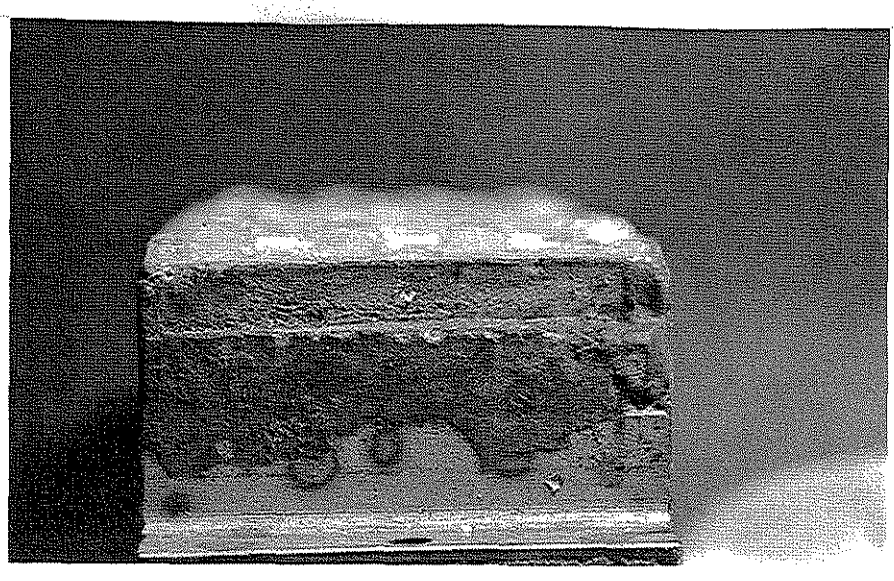

Figure 4.3 Sideways view of a serrated blade (0.5 in.) surface after a run

4.7 Ice Thickness Effect

Thickness effect was an important aspect in this research because, in natural conditions, roads may be covered by various ice thicknesses. Figures 3.11 through 3.20 indicate that both the maximum and average scraping forces reach their maximum value at a thickness range of 0.4 to 0.6 in.. As thickness increases above 0.6 in., the average reaction forces decrease. This is due to the fact that as the thickness increases, the likelihood of ice chipping off the concrete also increases. It was observed during this study that for larger thicknesses, ice was removed in bigger chunks leaving more bare concrete. This tendency to chip at higher ice thicknesses reflects the increased likelihood under such conditions a crack in the ice propagating for at least some distance along the ice-concrete interface or within the ice, rather than going directly to a free surface.

4.8 Velocity Effect

Two blades were tested with respect to forces and velocity, a serrated blade, with a tooth size of 0.25, and a classical blade, with rake angle 30° and clearance angle 5°. In both cases, it was shown (see Figures 3.21 through 3.24) that as the velocity increased, both vertical and horizontal reaction forces decreased. As these figures indicate, the maximum force was reached at a velocity of approximately 10 ft/s (6.8 mph). When the velocity doubles, the average vertical and horizontal forces decrease by about 50 lbs. As with thickness effect, it was observed that with increasing velocity more ice was chipped off the concrete block.

4.9 The Ice Scraping Process and Serrated Blades

From the tests conducted in this study, a picture of the processes involved in scraping ice from pavements has emerged. This is shown schematically in Figure 4.4.

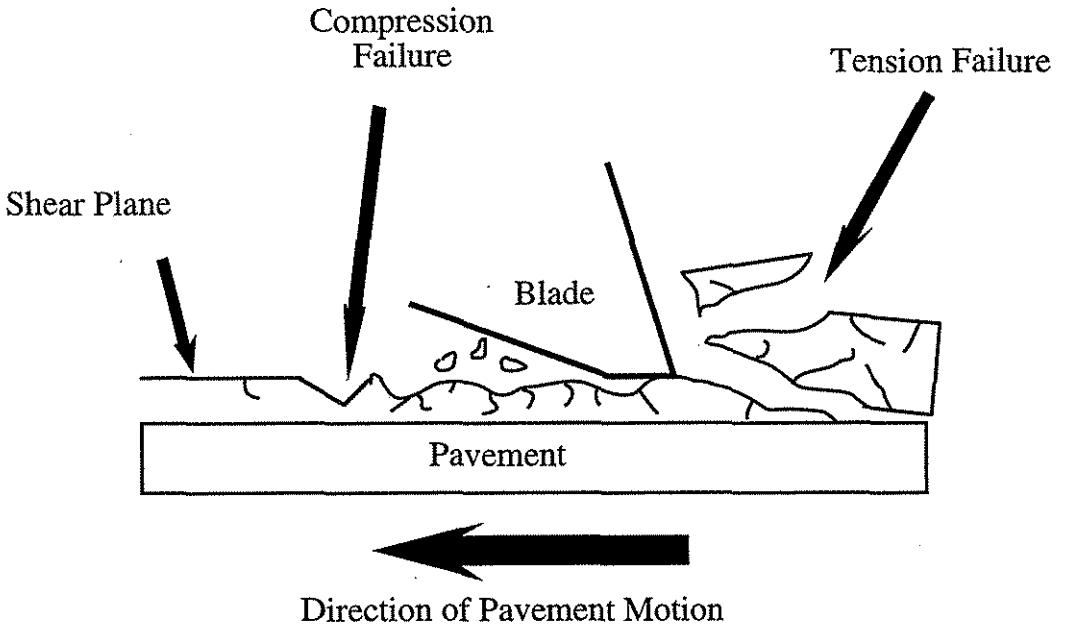

Figure 4.4 Ice failure modes

The processes include pulverization of the ice into small fragments which are both ejected in front of the blade, and recompressed beneath the blade and ejected behind it. Under certain conditions (thicker ice and higher velocities) cracks may propagate significant distances within the ice or along the ice-concrete interface, causing chipping of the ice. Chipping is preferable to pulverization of the ice because it is much less energy intensive, and would thus require lower scraping loads. However, methods which promote chipping have yet to be determined.

The test results obtained indicate that serrated blades are capable of removing ice at lower loads that "classical" or un-serrated blades. Further, the finer toothed blades were more efficient at removing ice than were the coarse blades. To that extent, it would seem that finely toothed blades should be considered for field testing. However, the step from the laboratory to the field is not straight forward and some care is needed in this regard.

Chapter 5
Conclusions

The primary objectives of this study were to develop an understanding of the ice scraping process and to investigate the effectiveness of serrated blades for ice scraping. The classical blades were used as the point of reference. The objective of this study was to investigate blade geometry in order to a) minimize horizontal and vertical scraping forces and b) maximize the ice removal.

The following points summarize the conclusions obtained from the research conducted in this study.

1. Various parameters of blades, such as rake angle, clearance angle, and flat width were tested. As a result of this study, it was shown that the blade with rake angle 30° and clearance angle 5° produced the minimum horizontal and vertical forces for varying ice thicknesses.
2. It was shown that velocity has an effect on the average value of scraping forces. As velocity increased beyond 10 ft/s, both average horizontal and vertical forces decreased.
3. As ice thickness increased beyond 0.5 inches, the average scraping forces significantly decreased (approximately 100 lbs).
4. The above observations correspond to an increase in ice chipping as thickness and velocity increase.
5. The study showed that serrated blades as opposed to non-serrated blades, required smaller forces to remove a given thickness of ice. There was, however, a slight reduction in the amount of ice that was removed with serrated blades. The difference in reaction forces between these two types of blades became smaller as the tooth size decreased.
6. The rate of ice removal of the serrated blades increased as the tooth size became smaller. It was a speculation, therefore, that the serrated blades might perform significantly better than the classical blades especially when the flat width increased due to wear.

A good picture of the ice scraping process has been developed from this study. From this, two challenges can be identified:

1. When ice is chipped, rather than pulverized, scraping loads are significantly (an order of magnitude) lower and more pavement is exposed. The challenge is to identify means to promote chipping of ice rather than pulverization.
2. Serrated blades appear capable of removing as much ice as classical blades but at lower loads. This suggests field tests would be valuable, and preliminary results in that direction are promising. This may be an area which warrants further study.

Bibliography

Bregman, J.J. Corrosion Inhibitors, 1st edition, New York: Macmillan Co., 1963.

Brohom, D.R. and S. Cohen, Maintenance Operations Office, Maintenance Branch, Ontario Ministry of Transportation and Communications, Downsview, Ontario.

Bruss, Poul T. "The Use of Stress Waves In Removing Ice From Concrete", Snow Removal and Ice Control Technology, Third International Symposium on Snow Removal and Ice Control Technology, September, 1992.

Chung, Cheng-Hua. "Development of Cutting Edges for Ice Removal from Pavements", Thesis submitted to the University of Iowa, May 1992.

Dickinson, W.E. (1968). "Snow and Ice Control-A Critical Look at Its Critics", Highway Research Record Number 227, Highway Research Board, National Research Council, Washington D.C.

Forkenbrock, David J., Norman S. J. Foster, and Michael C. Crum. 1994. *Transportation and Iowa's Economic Future*. Report prepared for the U.S. Department of Transportation and the Iowa Department of Transportation. Iowa City, IA: University of Iowa Public Policy Center.

Frederking, R. "Mechanical Properties of Ice and Their Application to Artic Ice Platforms", *Ice Tech 75*, The Society of Naval Architects and Marine Engineers, New York, 1975.

Fromm, H.J. (1968). "Corrosion of Auto-Body Steel and the Effects of Inhabited Deicing Salts", Highway Research Record Number 227, Highway Research Board, National Research Council, Washington D.C.

Hansen, Andrew C. "An Analysis of Energy Dissipation Caused by Snow Compaction During Displacement Flowing", SHRP Contract H-206, University of Wyoming, Laramie, November, 1990.

Hanbali, R. 1994. *The Economic Impact of Winter Road Maintenance on Road Users.* Paper No. 940191. Presented at 73rd Annual Meeting of the Transportation Research Board, January 9–13, 1994, Washington DC.

Hegmon, R.R. and W.E. Meyer. (1968). "The Effect of Antiskid Materials", Highway Research Record Number 227, Highway Research Board, National Research Council, Washington D.C.

Iowa DOT, etal. "Deicing Practices in Iowa: An Overview of Social, Economic and Environmental Implications, Prepared for The Iowa General Assembly House of Representatives, January, 1980.

Kinsey, J.S. etal. "Guidance Document for Selecting Antiskid Materials Applied to Ice- and Snow Covered Roadways", Report to United States Environmental Protection Agency, Iowa City, 1990.

Michel, B and R.O. Ramseier. "Classification of Riven and Lake Ice Based on Its Genesis, Structure and Texture", Depart. De Genie Civil, Universite Laval, Quebec, 1969.

Minsk, D.L. (1968). "Electrically Conductive Asphalt for Control of Snow and Ice Accumulation", Highway Research Record Number 227, Highway Research Board, National Research Council, Washington D.C.

Minsk, D.L. "Non corrosive Methods of Ice Control", Rpt. US. Army Cold regions Research and Engineering Laboratory, 1979

Murry, D.M. and M.R. Eigerman. (1972). "A Search: New Technology for Pavement Snow and Ice Control", EPA-R2-72-125, Office Of Research and Monitoring, U.S. Environmental Protection Agency, Washington D.C., December, 1972.

Nixon, Wilfrid A. "Improved Cutting Edges for Ice Removal", SHRP-H-346, National Research Council, Washington D.C., 1993.

Nixon, Wilfrid A. And Todd R. Frisbie. "Field Measurements of Plow Loads During Ice Removal Operations", Iowa Department of Transportation Project HR 334, Iowa Institute of Hydraulic Research, November, 1993.

W.A. Nixon and J.D. Potter, "Measurements of Ice Scraping Loads on Underbody Plows during Service Operations", Proc. 4th Ontl. Symposium on Snow Removal and Ice Control technology, TRB/NRC Paper No. D-4, Vol II, Reno, Nevada, August 1996.

Osborne, Mark D., "An Abrasive Air Blast System for Disbonding Ice and Snow From Pavement", Snow Removal and Ice Control Technology, Third International Symposium on Snow Removal and Ice Control Technology, September, 1992.

Sayles, F.H,. etal., "Classification and Laboratory Testing of Artificially Frozen Ground." Journal of Cold Regions Engineering, Vol. 1 No. 1, March 1987, P. 22-48.

SHRP. "Ice-Pavement Bond Disbonding-Surface Modification and Disbonding", Report Number SHPR-H/FR-90-2, National Research Council, Washington D.C., 1990.

SHRP. "Testing Program for the Experimental Plow", SHRP Contract H-206, University of Wyoming, Laramie, November, 1990.

Tabler, Ronald D. "Engineering the Control of Blowing Snow", SHRP Contract H-206, University of Wyoming, Laramie, November, 1990.

Transportation Research Board. 1992. *Highway Deicing: Comparing Salt and Calcium Magnesium Acetate*. Special Report 235, Washington DC: Transportation Research Board.

Wade, R.G. et al. "Improvements in Icebreaking by Use of Air Cushion Technology", Ice Tech 75, The Society of Naval Architects and Marine Engineers, New York, 1975.

Weber, Larry. "A Study of Fracture Toughness and Fatigue of Freshwater Ice", Thesis submitted to University of Iowa, May 1993.

Transportation Research Board. 1992. *Highway Deicing: Comparing Salt and Calcium Magnesium Acetate*. Special Report 235, Washington DC: Transportation Research Board.

Appendix A
Experimental Results

The results in this appendix were classified according to the amount of scatter produced from the reaction forces.

VG	-	very good (minimal scatter of data)
G	-	good (small scatter)
M	-	medium scatter
D	-	drop in forces
DD	-	double drop in forces

Clearance Angle 5°, Rake Angle 0°, Blade Width 3.21 in.

Cl	Run no.	Thic. in.	Vel ft/s	Max. H lbs	Avg. H lbs	Std. Dev.	Max. V lbs	Avg. V lbs	Std. Dev.
G	2	0.25	10	272	104	53	475	320	124
M	3	0.15	10	430	95	67	434	254	105
D	4	0.30	4	309	127	62	452	232	109
M	5	0.20	4	264	114	52	502	305	129
DD	6	0.25	4	360	74	86	534	151	161
G	7	0.25	4	230	104	51	527	318	151
G	8	0.25	4	166	81	33	495	298	99
G	9	0.25	7	264	74	37	450	235	76
M	10	0.25	7	211	84	44	672	255	150
D	11	0.35	7	365	99	59	511	227	109
M	12	0.30	7	264	68	43	472	264	110

Clearance Angle 5°, Rake Angle 0°, Flat Width 0 in.

Cl	Run no.	Thic. in.	Vel ft/s	Max. H lbs	Avg. H lbs	Std. Dev.	Max. V lbs	Avg. V lbs	Std. Dev.
M	1	0.30	10	326	79	67	360	144	122
D	2	0.30	10	367	59	65	287	56	66
M	3	0.35	9	283	95	69	278	184	108
DD	4	0.30	10	333	41	43	377	43	36
M	5	0.30	10	286	104	49	493	290	91
M	6	0.30	10	314	121	60	408	275	88
M	7	0.30	9	403	124	71	509	250	114
M	8	0.15	9	234	67	55	487	195	67
M	9	0.15	8	259	99	38	555	360	67
D	10	0.25	8	235	69	50	491	183	106
M	11	0.20	6	255	107	46	504	364	55
G	1	0.30	9	151	84	27	522	405	75
G	2	0.25	9	213	110	36	432	318	57
G	3	0.25	9	210	106	42	505	343	73
D	4	0.25	9	362	81	50	402	182	97
G	5	0.20	9	290	12	52	538	381	100
G	6	0.10	10	183	77	27	439	333	49
M	7	0.15	10	264	75	44	503	252	103
G	8	0.15	10	186	74	28	519	342	95
G	9	0.15	9	214	112	34	601	396	100
G	10	0.10	10	214	99	28	566	411	75
G	11	0.15	9	242	131	40	548	426	59
D	12	0.15	10	211	88	50	537	256	135
M	1	0.30	10	307	141	59	523	335	92
D	2	0.40	10	294	95	67	519	187	125
M	3	0.50	10	403	92	66	441	199	103
M	4	0.35	9	392	120	68	644	331	127
DD	5	0.55	8	504	84	90	400	129	104
M	6	0.45	10	360	86	82	405	105	95
DD	7	0.35	10	356	100	68	572	179	97
M	8	0.30	9	317	130	51	572	330	81
M	9	0.40	10	305	112	73	3499	168	92
M	10	0.40	8	407	135	71	507	294	109
D	11	0.35	8	315	101	62	460	212	106
D	12	0.35	7	350	61	68	408	122	116
M	1	0.10	10	183	76	25	650	404	80
G	2	0.10	5	205	66	34	556	210	92
G	3	0.10	10	170	86	27	545	389	67
G	4	0.15	5	210	116	26	621	443	52
G	5	0.15	5	206	102	29	541	394	50
G	6	0.15	3	206	64	25	559	309	141
D	7	0.35	11	359	103	75	585	145	129
M	8	0.30	11	288	105	65	542	184	116
M	9	0.40	9	493	106	103	403	162	131

M	10	0.50	10	392	136	76	406	245	88
G	11	0.40	5	545	90	71	387	200	55
D	12	0.40	5	382	146	74	559	317	98
DD	1	0.35	11	423	74	80	531	158	172
DD	2	0.35	8	367	40	69	242	26	51
D	4	0.40	11	274	72	61	377	122	100
D	5	0.30	8	436	45	55	317	25	33
D	6	0.50	10	263	92	70	268	68	58
M	7	0.45	8	377	81	73	269	65	50
DD	8	0.45	9	357	81	73	430	97	102
M	11	0.50	8	307	126	66	505	266	76

Clearance Angle 5°, Rake Angle 15°, Flat Width 0 in.

Cl	Run no.	Thic. in.	Vel ft/s	Max. H lbs	Avg. H lbs	Std. Dev.	Max. V lbs	Avg. V lbs	Std. Dev.
D	2	0.45	10	223	75	50	353	188	103
M	3	0.60	10	177	57	50	220	98	72
D	4	0.50	10	183	68	37	473	173	115
M	5	0.45	10	257	79	43	476	210	122
D	6	0.50	10	202	68	45	513	187	132
D	7	0.55	10	234	71	47	486	199	114
DD	8	0.45	10	210	75	46	523	242	136
DD	9	0.45	10	193	48	52	249	34	43
G	10	0.55	10	166	76	28	519	319	84
DD	11	0.45	10	190	60	48	506	127	148
D	12	0.45	10	216	64	54	474	171	151
G	1	0.30	10	177	88	40	539	360	135
DD	2	0.25	10	201	61	39	561	175	127
D	3	0.45	10	218	73	35	590	280	129
G	4	0.20	10	146	81	23	524	328	88
G	5	0.25	10	208	96	32	579	362	67
G	6	0.25	10	198	95	33	526	387	97
G	7	0.50	10	161	76	32	481	330	100
G	8	0.25	10	185	89	34	526	345	101
G	9	0.30	10	210	94	32	538	370	93
G	10	0.25	10	201	91	26	570	365	67
M	11	0.35	10	176	92	32	558	344	90
D	12	0.35	10	173	79	44	530	249	144
M	1	0.10	10	122	60	23	492	270	97
M	2	0.30	10	170	71	30	524	241	78
M	3	0.15	10	129	71	22	495	321	39
M	4	0.20	10	154	67	30	494	271	95
M	5	0.15	10	127	69	23	431	280	81
G	6	0.20	10	165	70	26	459	251	50
M	7	0.15	10	154	61	29	568	288	121
M	1	0.25	10	165	80	24	440	296	90
M	2	0.30	10	183	78	54	464	284	82
D	3	0.20	10	181	68	44	494	238	104
D	4	0.30	10	250	63	34	457	298	110
G	5	0.40	10	339	112	35	422	366	25
G	6	0.30	10	273	98	42	425	300	33
DD	7	0.30	10	198	88	32	484	199	140
G	8	0.30	10	188	87	28	480	338	44
D	9	0.30	10	259	51	44	233	103	110
M	10	0.25	10	138	75	25	478	315	65
G	11	0.25	10	195	94	25	493	317	55
D	12	0.25	10	206	86	27	482	299	78
M	1	0.30	10	140	64	36	517	243	129
G	2	0.20	10	162	55	30	524	221	87

D	3	0.20	10	133	69	23	538	321	76
M	4	0.25	10	175	70	35	534	278	118
G	5	0.25	10	188	74	38	597	292	126
G	6	0.15	10	146	66	24	525	294	56
M	7	0.25	10	163	58	29	383	238	84
M	8	0.20	10	182	73	32	586	349	110
D	9	0.20	10	208	58	27	539	249	129
D	10	0.30	10	233	67	41	542	259	130
G	11	0.20	10	177	84	26	580	385	80
M	12	0.20	10	152	69	33	539	311	109
D	1	0.30	17	349	219	69	452	209	124
D	3	0.35	17	463	258	86	489	228	110
M	4	0.30	17	344	243	56	451	234	101
M	5	0.35	17	389	242	81	433	237	112
M	6	0.30	17	371	213	67	428	204	100
M	7	0.25	17	417	255	96	791	267	114
M	8	0.25	17	368	206	112	485	198	114
M	9	0.25	17	378	187	99	519	204	111
M	10	0.20	17	404	225	96	383	207	112
M	11	0.35	17	360	213	100	393	178	100
D	12	0.25	17	361	185	113	459	180	149

Clearance Angle 5°, Rake Angle 30°, Flat Width 0 in.

Cl	Run no.	Thic. in.	Vel ft/s	Max. H lbs	Avg. H lbs	Std. Dev.	Max. V lbs	Avg. V lbs	Std. Dev.
M	1	0.40	10	142	81	29	141	77	37
M	2	0.30	10	153	85	33	161	84	43
DD	3	0.35	10	170	59	42	180	51	49
DD	4	0.35	17	156	59	35	118	30	37
M	6	0.25	17	178	83	27	175	65	50
D	7	0.25	19	150	83	45	143	58	57
M	8	0.25	19	201	118	40	164	96	45
M	9	0.30	20	149	89	39	204	68	55
D	10	0.25	23	143	75	40	106	25	52
M	11	0.45	23	206	87	55	210	8	52
D	12	0.20	23	162	91	50	175	82	64
M	1	0.15	10	117	73	20	148	99	22
M	2	0.20	10	130	81	19	158	100	23
M	3	0.25	10	126	68	20	130	79	22
M	4	0.15	17	156	74	26	122	81	30
M	5	0.10	17	118	69	25	140	91	30
M	6	0.15	17	118	68	21	147	82	33
D	7	0.10	20	129	59	26	140	51	29
M	8	0.15	20	123	74	27	145	80	35
D	9	0.20	20	164	81	32	172	53	34
D	10	0.20	23	120	74	28	151	62	40
DD	11	0.15	23	148	56	34	139	22	64
M	1	0.45	10	165	107	26	181	125	37
D	2	0.60	10	156	80	35	131	70	46
M	3	0.50	10	147	88	26	156	90	41
M	4	0.50	17	163	78	40	137	70	46
D	5	0.35	17	154	78	36	154	61	47
D	6	0.40	17	157	97	37	150	84	40
D	7	0.40	20	174	85	43	139	72	43
M	8	0.45	20	174	92	43	172	86	60
M	9	0.40	20	204	98	45	204	94	57
D	10	0.45	23	241	90	54	199	75	58
D	11	0.35	23	131	69	37	128	31	64
D	12	0.35	23	142	76	43	149	63	44
M	4	0.41	9	401	284	76	621	417	116
G	5	0.40	9	463	361	59	702	555	91
D	6	0.30	9	477	330	110	763	515	186
D	7	0.35	9	485	313	88	683	462	161
G	8	0.30	9	477	411	24	755	653	34
M	9	0.25	9	425	308	62	641	443	124
D	10	0.35	8	484	354	114	757	528	188
VB	11	0.35	8	522	457	20	846	726	44
M	12	0.25	9	525	405	60	875	660	111

Clearance Angle 5°, Rake Angle 45°, Blade Width 0 in.

Cl	Run no.	Thic. in.	Vel ft/s	Max. H lbs	Avg. H lbs	Std. Dev.	Max. V lbs	Avg. V lbs	Std. Dev.
M	1	0.45	19	125	77	24	214	131	55
DD	2	0.45	22	133	35	34	220	62	78
M	3	0.50	21	143	74	25	350	190	75
DD	4	0.45	23	169	43	38	360	123	132
M	5	0.40	22	141	73	27	368	201	59
G	6	0.40	21	133	83	18	457	345	35
M	7	0.40	22	155	77	24	461	350	98
M	8	0.35	22	117	67	18	471	299	62
G	9	0.35	23	128	81	27	450	283	90
M	10	0.35	22	144	78	26	332	241	52
D	11	0.50	23	145	62	35	365	181	11
M	12	0.45	24	118	68	32	335	192	88
G	1	0.35	6	104	52	22	173	112	40
M	2	0.35	6	119	69	26	457	364	137
G	3	0.30	6	150	60	24	359	276	96
M	4	0.30	9	158	63	24	442	270	76
G	5	0.25	9	114	68	16	381	280	30
M	6	0.10	9	118	62	18	389	297	48
G	7	0.20	9	148	69	16	419	262	36
M	8	0.20	9	128	90	23	435	285	70
G	9	0.20	9	123	56	18	309	214	40
M	10	0.20	10	115	64	21	305	207	34
M	11	0.20	10	119	67	23	420	263	82
G	12	0.20	4	150	66	26	390	299	126

Clearance Angle 5°, Rake Angle 30°, Blade Width 0.125 in.

Cl	Run no.	Thic. in.	Vel ft/s	Max. H lbs	Avg. H lbs	Std. Dev.	Max. V lbs	Avg. V lbs	Std. Dev.
M	4	0.30	10	426	227	60	2265	1181	432
G	5	0.20	10	507	245	58	2268	1343	317
M	6	0.15	10	403	241	44	2268	1354	379
M	7	0.15	10	508	309	76	2268	1452	340
M	8	0.15	10	491	243	74	2207	1254	376
M	9	0.20	10	426	227	60	2265	1181	432
M	10	0.15	10	477	187	67	2268	1175	486
M	11	0.20	10	310	200	99	2268	1249	330
M	12	0.25	10	648	224	85	2268	1219	601
M	1	0.20	10	533	256	142	2268	912	390
M	2	0.35	10	806	384	109	1498	633	217
M	3	0.30	10	785	556	80	1419	917	199
M	4	0.20	10	652	484	78	1193	730	196
M	5	0.20	10	684	563	68	1145	907	153
M	6	0.20	10	782	579	94	1450	942	230
M	7	0.20	10	794	545	95	1509	873	200
M	8	0.20	10	703	436	67	1273	773	139
D	9	0.30	10	907	460	182	1754	830	333
G	10	0.25	10	771	600	47	1417	1049	132
G	11	0.20	10	799	407	64	1407	964	162
M	12	0.20	10	599	743	83	1081	607	188
M	1	0.25	10	1002	563	115	2085	1265	315
M	2	0.20	10	877	593	86	1687	1172	183
M	3	0.15	10	780	598	100	1498	990	282
M	4	0.25	10	790	539	124	1415	969	265
M	5	0.15	10	780	604	95	1471	857	257
M	6	0.20	10	836	674	102	1668	1031	270
M	7	0.20	10	953	672	121	1811	1169	301
M	8	0.20	10	857	597	115	1533	982	300
M	9	0.20	10	482	260	85	2101	1117	368
M	10	0.20	4	887	623	115	1746	1024	357
M	11	0.15	10	888	591	113	1784	979	343
M	12	0.15	10	791	438	99	1413	686	244

Clearance Angle 5°, Rake Angle 30°, Blade Width 0.3 in.

Cl	Run no.	Thic. in.	Vel ft/s	Max. H lbs	Avg. H lbs	Std. Dev.	Max. V lbs	Avg. V lbs	Std. Dev.
M	1	0.20	8	3095	2176	369	3392	2276	576
DD	2	0.30	8	2039	701	407	1958	636	451
M	3	0.50	8	1567	978	404	1508	850	367
DD	5	0.35	7	2749	1520	529	2522	1358	671
D	6	0.40	7	2145	1136	619	2191	1040	625
M	7	0.35	8	2761	1739	824	2477	1501	777
D	8	0.35	7	2838	1366	571	2642	1202	633
D	9	0.30	7	2440	1256	629	2472	1200	686
M	10	0.20	7	2889	1763	493	2655	1564	525
DD	11	0.25	2	2228	251	322	2206	220	295
D	12	0.10	6	2701	1535	671	2545	1394	661
D	2	0.30	5	2601	1267	586	2539	1072	659
D	3	0.30	5	2099	1127	358	2703	1407	557
D	4	0.25	5	1952	953	469	2748	1280	715
D	5	0.25	5	2136	1100	364	2715	1398	569
D	6	0.25	7	1807	1122	286	2623	1458	535
D	7	0.25	8	1814	843	354	2624	1144	561
M	8	0.20	8	1419	930	168	2037	1249	321
M	9	0.20	7	2138	1377	273	2713	1706	494
D	10	0.20	8	2139	972	394	2781	1315	630
D	11	0.20	9	1856	838	299	2655	1150	498
D	12	0.20	8	2316	1256	387	2977	1458	548
M	1	0.20	7	1249	753	178	2052	1098	247
D	2	0.25	6	1117	490	355	1643	654	501
M	3	0.40	7	1163	952	369	1623	1028	511
D	4	0.40	6	1755	732	378	2601	913	593
D	5	0.40	6	1765	525	475	2379	768	612
D	6	0.30	5	2146	813	539	2761	1011	910
D	7	0.30	5	1756	880	371	2601	1099	507
D	8	0.30	4	1673	903	343	2589	1264	655
D	10	0.20	7	1510	594	524	2171	813	701
D	11	0.30	6	1226	719	272	1621	958	401

Clearance Angle 5°, Rake Angle 30°, Blade Width 0.4 in.

Cl	Run no.	Thic. in.	Vel ft/s	Max. H lbs	Avg. H lbs	Std. Dev.	Max. V lbs	Avg. V lbs	Std. Dev.
M	1	0.40	7	2115	1174	611	2598	1532	820
M	2	0.40	7	1985	1354	422	2585	1489	351
M	3	0.30	5	2027	1480	151	2620	1748	372
M	4	0.35	5	2254	1268	269	2780	1487	441
M	5	0.35	5	2897	1675	735	3091	1961	854
D	6	0.40	5	2031	1143	559	2582	1429	801
D	7	0.35	5	3093	1097	998	3387	1144	895
M	8	0.10	5	2443	1577	630	2765	1890	818
D	9	0.30	5	2636	764	727	3005	934	981
M	11	0.05	5	2768	1432	727	2887	1817	770
D	12	0.25	5	2292	781	626	2751	1043	837
D	1	0.40	7	3012	1613	988	3082	1075	832
D	3	0.35	7	2873	685	750	2635	653	733
D	4	0.40	7	4520	782	984	3211	541	930
D	5	0.45	7	4217	1096	958	3381	861	998
D	6	0.45	7	3637	4590	999	2887	1340	944
DD	7	0.50	7	3292	1243	998	2650	1106	988
M	8	0.30	7	2696	1355	936	2630	1317	840
D	9	0.25	7	3140	1360	999	2713	1152	996
M	10	0.35	7	3431	1713	978	6058	1454	973
D	11	0.30	7	3623	1355	994	2942	1232	998
M	12	0.40	7	3698	1531	993	2848	1370	951
DD	1	0.30	5	3060	1718	559	4530	1525	540
M	2	0.20	5	2133	1424	247	2122	1402	259
M	3	0.35	5	3820	1931	728	2906	1649	544
M	4	0.35	5	3226	1915	498	2718	4724	467
M	5	0.35	5	3525	1783	542	2826	4622	510
M	6	0.35	5	2799	1504	362	2542	1380	391
M	7	0.30	7	3217	1990	909	2678	1750	825
M	8	0.30	7	3262	1752	950	2648	4789	907
M	9	0.30	7	3835	2049	996	2864	1814	862
M	10	0.40	7	2735	1761	786	2590	1627	747
DD	11	0.20	7	2970	786	718	2609	789	738
M	12	0.30	7	3060	2102	883	2681	1820	798

Clearance Angle 2°, Rake Angle 30°, Blade Width 0 in.

Cl	Run no.	Thic. in.	Vel ft/s	Max. H lbs	Avg. H lbs	Std. Dev.	Max. V lbs	Avg. V lbs	Std. Dev.
G	1	0.35	7	422	290	81	407	304	76
G	2	0.25	7	434	335	42	411	342	37
VG	3	0.30	7	129	351	123	451	373	117
G	4	0.30	7	441	365	67	456	386	60
G	5	0.30	7	504	326	177	514	344	175
M	6	0.20	7	442	308	140	455	321	71
M	7	0.30	7	462	309	125	494	332	125
G	8	0.30	7	460	397	62	989	419	48
M	9	0.25	9	455	314	79	502	341	79
VG	10	0.20	3	513	438	14	572	495	16
VG	11	0.30	3	603	540	25	687	614	31
VG	12	0.35	3	573	500	24	646	574	30
G	1	0.20	8	365	261	25	575	369	43
VG	3	0.15	8	476	407	21	805	683	37
VG	4	0.20	8	488	409	22	782	659	41
G	5	0.15	8	573	179	30	986	825	60
M	6	0.25	8	458	367	47	727	560	102
M	7	0.20	8	454	338	48	739	533	86
VG	8	0.25	7	495	389	21	796	620	39
VG	9	0.10	7	595	495	31	1003	842	46
VG	10	0.20	7	587	475	24	948	785	41
G	11	0.10	7	481	241	107	744	378	180
M	12	0.20	7	522	414	75	898	683	137
G	1	0.20	8	368	313	23	567	480	35
M	2	0.30	8	425	317	51	679	494	82
G	3	0.20	8	445	351	49	729	555	74
G	4	0.35	8	470	390	29	722	604	48
G	5	0.20	8	400	327	39	639	518	55
VG	6	0.20	8	619	532	33	1054	916	57
D	7	0.30	9	463	307	106	692	451	157
VG	8	0.15	8	465	405	22	770	678	34
DD	9	0.25	9	378	195	94	587	288	158
G	11	0.25	9	539	476	24	887	761	48
D	12	0.25	9	525	387	134	852	632	225
DD	2	0.45	7	403	119	106	619	170	177
D	3	0.45	8	456	217	87	699	307	124

Clearance Angle 10° Rake Angle 30°, Blade Width 0 in.

Cl	Run no.	Thic. in.	Vel ft/s	Max. H lbs	Avg. H lbs	Std. Dev.	Max. V lbs	Avg. V lbs	Std. Dev.
M	2	0.40	7	340	184	84	214	85	57
DD	3	0.45	7	328	70	115	190	25	66
D	4	0.45	7	357	177	100	185	79	57
M	5	0.45	7	304	180	54	209	118	38
M	6	0.25	7	320	173	62	223	107	45
M	7	0.35	7	356	224	99	210	115	56
M	8	0.30	7	355	245	65	207	130	36
M	9	0.30	7	361	252	71	206	147	41
M	10	0.30	7	300	165	58	181	104	37
M	11	0.30	7	321	148	70	191	95	36
M	1	0.20	4	324	193	87	219	130	60
M	2	0.20	4	337	189	76	216	129	51
D	3	0.40	4	361	209	100	221	126	62
D	4	0.20	4	321	182	91	221	117	66
D	5	0.25	4	374	218	107	262	126	64
D	6	0.40	4	361	225	102	244	135	69
M	7	0.20	4	404	212	97	212	134	62
D	8	0.20	10	339	148	98	213	102	65
D	9	0.20	10	343	149	105	206	85	70
M	10	0.15	10	322	170	104	212	110	71
M	11	0.15	10	341	186	118	253	122	74
D	12	0.20	13	343	149	104	222	93	76
D	1	0.30	13	333	203	60	232	108	53
D	2	0.35	13	342	180	74	205	85	70
DD	3	0.35	15	410	151	117	242	69	89
D	4	0.35	15	355	154	74	182	65	61
D	5	0.30	15	337	205	51	276	119	52
D	6	0.20	15	314	171	40	182	107	41
D	7	0.20	20	249	128	90	176	80	63
M	8	0.20	20	331	175	98	234	108	72
D	9	0.25	20	289	153	93	230	85	80
D	10	0.25	20	338	184	105	235	103	67
D	11	0.25	20	294	159	101	220	83	62
D	12	0.30	20	355	131	105	222	66	75

Clearance Angle 5°, Rake Angle 30°, Blade Width 0.125 in.

Cl	Run no.	Thic. in.	Vel ft/s	Max. H lbs	Avg. H lbs	Std. Dev.	Max. V lbs	Avg. V lbs	Std. Dev.
M	1	0.40	11	185	112	37	253	171	58
M	2	0.40	10	173	113	37	280	169	54
M	3	0.35	10	153	115	26	291	181	39
M	4	0.35	17	209	113	37	251	159	59
M	5	0.40	17	187	124	46	267	154	64
D	6	0.50	17	193	80	46	198	66	55
D	7	0.35	20	184	98	50	237	102	75
G	8	0.30	20	170	122	39	274	186	54
M	9	0.40	20	189	111	47	233	139	69
M	10	0.40	23	213	122	44	276	136	73
M	11	0.35	23	183	116	49	276	129	79
G	12	0.35	23	196	112	48	290	144	68
M	1	0.10	10	130	86	22	242	147	40
M	2	0.20	10	122	76	23	285	137	49
M	3	0.15	10	152	85	32	313	156	65
M	4	0.15	17	138	87	36	244	133	56
M	5	0.15	17	159	92	31	299	153	55
M	6	0.15	17	133	88	32	212	141	48
M	7	0.15	16	135	93	29	216	140	37
M	8	0.10	16	141	88	33	213	138	47
M	9	0.15	20	152	74	30	228	98	56
M	10	0.15	23	118	80	31	219	122	39
M	11	0.15	23	155	101	38	224	161	51
M	1	0.55	10	196	101	54	283	161	85
M	2	0.65	10	182	54	53	247	80	80
D	3	0.60	10	195	89	58	280	138	100
D	4	0.60	10	197	82	50	327	146	85
M	5	0.60	19	281	138	70	304	184	98
D	7	0.50	17	185	96	54	255	114	76
D	8	0.60	20	216	92	70	316	79	89
D	9	0.65	19	175	66	66	218	56	62
D	10	0.60	23	226	112	65	274	99	92
D	11	0.60	23	237	117	69	239	133	61
D	12	0.60	23	194	114	62	265	130	82

Clearance Angle 5°, Rake angle 30°, Tooth Size 0.25 in.

Cl	Run no.	Thic. in.	Vel ft/s	Max. H lbs	Avg. H lbs	Std. Dev.	Max. V lbs	Avg. V lbs	Std. Dev.
M	1	0.25	4	201	111	29	207	100	37
M	2	0.3	4	187	97	32	241	115	43
D	3	0.3	4	221	74	56	224	83	63
M	4	0.4	4	221	134	58	216	138	71
D	5	0.25	4	180	77	37	194	85	40
M	6	0.25	4	213	139	54	235	156	72
M	7	0.3	7	246	161	44	268	179	48
M	8	0.35	7	174	113	23	206	129	28
M	9	0.25	7	212	146	26	310	177	34
M	10	0.25	7	203	130	26	210	151	28
M	11	0.35	7	165	114	29	270	134	40
D	12	0.25	7	203	123	39	309	154	58
DD	1	0.5	9	229	117	56	311	129	86
D	2	0.4	9	240	145	47	316	178	71
DD	3	0.4	9	233	47	61	350	32	77
M	4	0.3	8	266	165	61	359	209	87
M	5	0.3	9	281	133	50	424	167	78
M	6	0.3	10	301	190	43	431	247	75
D	7	0.35	13	296	142	83	423	180	111
D	8	0.3	13	209	107	55	350	135	80
M	9	0.3	13	262	169	86	373	214	111
D	10	0.4	12	252	147	72	325	170	95
M	11	0.35	12	251	165	66	357	210	81
D	12	0.3	12	276	168	89	364	209	116
M	1	0.35	17	267	161	57	272	178	60
M	2	0.35	17	289	179	51	338	201	51
M	3	0.3	16	245	129	57	296	145	77
M	4	0.35	15	279	147	60	330	175	80
M	5	0.25	16	306	161	60	453	205	70
M	6	0.3	16	247	158	40	379	198	68
M	7	0.3	17	320	150	86	437	193	103
M	8	0.25	17	312	139	68	432	170	81
M	9	0.25	17	285	154	63	507	195	81
M	10	0.25	17	258	156	57	388	181	65
M	11	0.35	17	273	154	78	310	155	79
M	12	0.25	18	273	158	67	450	192	84
M	2	0.25	17	211	125	60	297	156	74
M	3	0.35	18	266	123	67	354	137	97
M	4	0.35	19	295	106	71	340	105	77
M	5	0.3	19	212	100	64	297	117	72
M	6	0.3	18	290	137	75	481	176	115
M	7	0.3	20	279	127	82	394	159	104
M	8	0.25	18	240	140	61	320	180	84
M	9	0.25	19	277	121	86	449	143	105

M	10	0.25	18	239	150	73	420	186	92
M	11	0.25	18	304	145	80	490	176	87
M	12	0.25	19	286	166	77	479	217	102
M	1	0.5	13	316	174	64	414	227	95
D	2	0.4	13	324	184	73	518	261	117
M	3	0.55	15	359	158	66	497	226	94
DD	4	0.5	13	273	76	77	397	94	108
DD	5	0.5	15	330	150	97	553	171	127
DD	6	0.45	15	302	104	85	463	117	124
M	7	0.55	12	296	162	53	433	229	81
DD	8	0.45	15	335	81	91	418	62	118
M	9	0.5	15	297	114	77	418	132	87
D	10	0.35	14	311	161	53	568	243	119
M	11	0.5	14	293	131	79	336	126	90
DD	12	0.5	13	270	103	84	385	117	121
D	2	0.75	9	190	91	54	198	78	63
D	4	0.8	12	186	67	57	298	52	58
M	6	0.65	11	278	119	48	255	123	45
M	7	0.6	11	233	126	39	334	208	55
D	8	0.75	11	193	106	51	313	145	64
D	9	0.75	12	255	60	60	130	38	48
D	10	0.7	12	186	55	59	158	37	55
DD	11	0.7	11	145	32	48	244	25	71

Clearance Angle 5°, Rake Angle 30°, Tooth Size 0.5 in.

Cl	Run no.	Thic. in.	Vel ft/s	Max. H lbs	Avg. H lbs	Std. Dev.	Max. V lbs	Avg. V lbs	Std. Dev.
M	1	0.25	9	112	62	23	170	79	44
M	2	0.35	9	120	60	27	154	74	36
M	3	0.35	10	132	83	24	413	131	87
M	4	0.35	10	142	76	26	376	117	41
M	5	0.4	9	142	77	25	295	73	40
M	6	0.35	10	152	83	23	323	146	79
M	7	0.4	12	191	79	55	333	144	93
M	8	0.35	15	186	93	56	231	139	46
M	9	0.3	14	181	92	57	530	216	129
M	10	0.3	14	171	85	54	242	128	62
M	11	0.35	15	172	92	65	333	132	73
M	12	0.35	16	147	66	49	163	72	51
M	1	0.3	9	133	85	20	295	130	50
M	2	0.2	10	119	74	20	182	107	30
M	3	0.2	9	125	77	23	259	130	56
M	4	0.15	9	134	101	15	374	204	104
M	5	0.15	10	136	91	16	383	180	87
M	6	0.2	9	142	98	16	270	169	46
M	7	0.2	18	140	82	43	291	161	58
M	8	0.15	17	157	105	32	275	141	46
M	9	0.15	16	135	89	23	127	88	22
M	11	0.15	18	150	79	29	243	109	48
M	1	0.15	24	112	37	39	123	39	37
M	2	0.15	24	130	63	45	112	46	44
M	3	0.15	24	107	56	38	142	58	44
M	4	0.2	24	117	57	39	148	63	47
M	5	0.2	24	144	72	51	181	82	50
M	6	0.25	24	144	67	47	189	94	53
M	7	0.35	25	217	107	77	298	143	76
M	8	0.25	24	162	85	59	238	125	75
M	9	0.15	24	123	56	41	137	66	50
M	10	0.25	20	167	106	44	261	142	48
M	11	0.15	24	126	69	47	232	113	65
M	12	0.3	24	166	89	59	274	140	71

Clearance Angle 5°, Rake Angle 30°, Tooth Size 1 in.

Cl	Run no.	Thic. in.	Vel ft/s	Max. H lbs	Avg. H lbs	Std. Dev.	Max. V lbs	Avg. V lbs	Std. Dev.
M	3	0.25	24	101	63	18	135	62	26
M	4	0.15	24	79	47	17	97	63	17
M	5	0.25	24	118	51	25	109	24	33
M	6	0.2	24	99	67	18	145	88	24
M	7	0.1	17	78	41	12	103	53	29
M	8	0.15	17	73	29	13	99	46	19
M	9	0.1	17	92	49	15	117	62	28
M	10	0.05	17	70	46	16	130	80	25
M	11	0.05	17	61	40	11	96	68	18
M	12	0.1	17	65	34	16	89	48	22
M	2	0.35	10	133	68	22	131	78	28
M	3	0.4	10	118	56	24	113	49	32
M	4	0.35	11	138	61	26	159	67	36
M	5	0.35	17	140	65	29	129	44	46
M	6	0.35	17	143	90	25	115	58	30
M	7	0.3	17	151	80	30	137	67	32
M	8	0.2	17	94	63	16	115	68	24
M	9	0.3	17	126	67	27	122	48	39
M	10	0.25	17	125	71	17	151	69	35
M	11	0.25	17	95	60	19	107	45	33
M	12	0.2	17	120	68	27	127	45	36
M	2	0.3	10	111	54	17	121	53	27
M	3	0.45	10	134	60	20	107	51	33
M	4	0.4	17	100	62	23	106	35	38
M	5	0.35	17	115	68	23	109	61	32
M	6	0.4	17	115	52	27	96	23	27
M	7	0.35	20	113	64	29	95	29	40
M	8	0.3	20	121	56	29	87	32	33
M	9	0.35	20	126	66	32	103	35	48
M	10	0.4	23	124	66	36	126	19	47
M	11	0.4	24	149	71	37	123	12	42
M	12	0.45	24	161	90	41	195	43	52